Today's outline - February 06, 2020

Today's outline - February 06, 2020

- Designing a multilayer

Today's outline - February 06, 2020

- Designing a multilayer
- Reflection from a graded index

Today's outline - February 06, 2020

- Designing a multilayer
- Reflection from a graded index
- Reflection from rough surfaces

Today's outline - February 06, 2020

- Designing a multilayer
- Reflection from a graded index
- Reflection from rough surfaces
- Surface models

Today's outline - February 06, 2020

- Designing a multilayer
- Reflection from a graded index
- Reflection from rough surfaces
- Surface models
- Reflectivity research topics

Today's outline - February 06, 2020

- Designing a multilayer
- Reflection from a graded index
- Reflection from rough surfaces
- Surface models
- Reflectivity research topics
- Mirrors

Today's outline - February 06, 2020

- Designing a multilayer
- Reflection from a graded index
- Reflection from rough surfaces
- Surface models
- Reflectivity research topics
- Mirrors

Homework Assignment #02:
Problems on Blackboard
due Tuesday, February 18, 2020

Multilayer design

Materials for multilayer monochromator chosen to reflect 12 keV x-rays at ~ 2 degrees with 0.5% and 1.0% bandwidth

A. Khounsary et al., "A dual-bandwidth multilayer monochromator system," *Proc. SPIE* **10760**, 107600j (2018).

Multilayer design

Materials for multilayer monochromator chosen to reflect 12 keV x-rays at ~ 2 degrees with 0.5% and 1.0% bandwidth

Common design parameters include bilayer filler fraction $\Gamma = 0.5$, roughness $\sigma = 0.35$ nm, and number of bilayers $N = 300$

A. Khounsary et al., "A dual-bandwidth multilayer monochromator system," *Proc. SPIE* **10760**, 107600j (2018).

Multilayer design

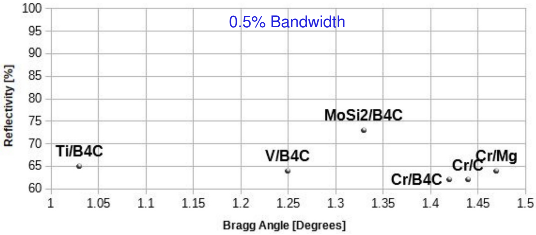

Materials for multilayer monochromator chosen to reflect 12 keV x-rays at ~ 2 degrees with 0.5% and 1.0% bandwidth

Common design parameters include bilayer filler fraction $\Gamma = 0.5$, roughness $\sigma = 0.35$ nm, and number of bilayers $N = 300$

A. Khounsary et al., "A dual-bandwidth multilayer monochromator system," *Proc. SPIE* **10760**, 107600j (2018).

Multilayer design

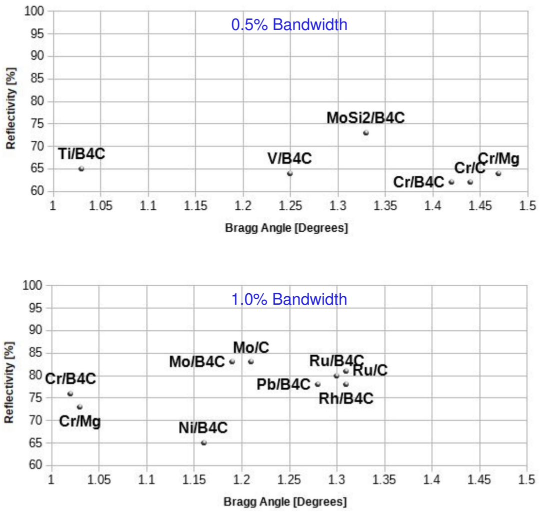

A. Khounsary et al., "A dual-bandwidth multilayer monochromator system," *Proc. SPIE* **10760**, 107600j (2018).

Materials for multilayer monochromator chosen to reflect 12 keV x-rays at ~ 2 degrees with 0.5% and 1.0% bandwidth

Common design parameters include bilayer filler fraction $\Gamma = 0.5$, roughness $\sigma = 0.35$ nm, and number of bilayers $N = 300$

Multilayer design

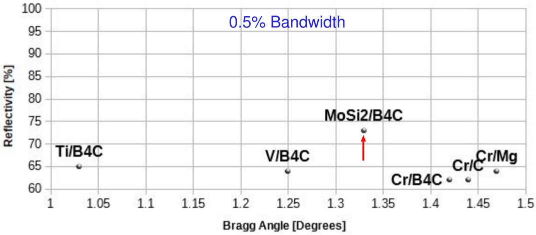

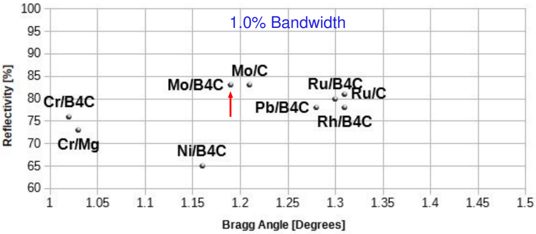

A. Khounsary et al., "A dual-bandwidth multilayer monochromator system," *Proc. SPIE* **10760**, 107600j (2018).

Materials for multilayer monochromator chosen to reflect 12 keV x-rays at ~ 2 degrees with 0.5% and 1.0% bandwidth

Common design parameters include bilayer filler fraction $\Gamma = 0.5$, roughness $\sigma = 0.35$ nm, and number of bilayers $N = 300$

$MoSi_2/B_4C$ and Mo/B_4C were selected for the 0.5% and 1.0% bandwidth coatings, respectively

Multilayer fabrication & testing

The 0.5% and 1.0% bandwidth layers were deposited side-by-side on a monolithic 20 mm × 30 mm × 100 mm polished silicon block

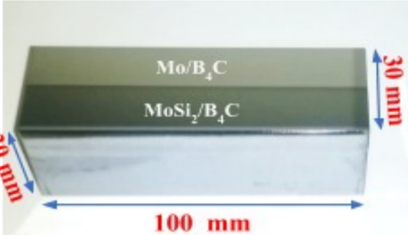

A. Khounsary et al., "A dual-bandwidth multilayer monochromator system," *Proc. SPIE* **10760**, 107600j (2018).

Multilayer fabrication & testing

The 0.5% and 1.0% bandwidth layers were deposited side-by-side on a monolithic 20 mm × 30 mm × 100 mm polished silicon block

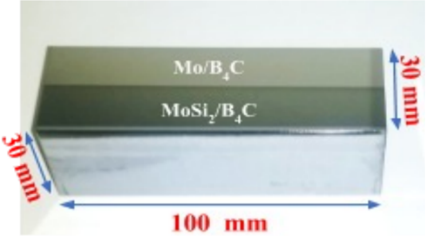

When illuminated with 12 keV x-rays the two multilayers showed diffraction peaks at nearly the same angle. The reflectivities were both over 75% and the bandwidths were 0.52% and 0.86%, respectively.

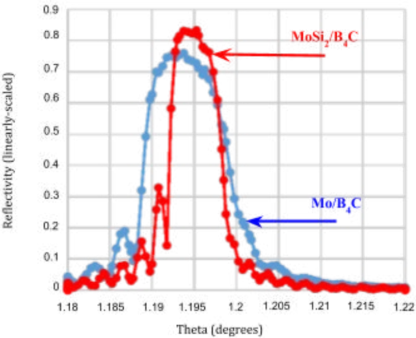

A. Khounsary et al., "A dual-bandwidth multilayer monochromator system," *Proc. SPIE* **10760**, 107600j (2018).

Multilayer spectrum

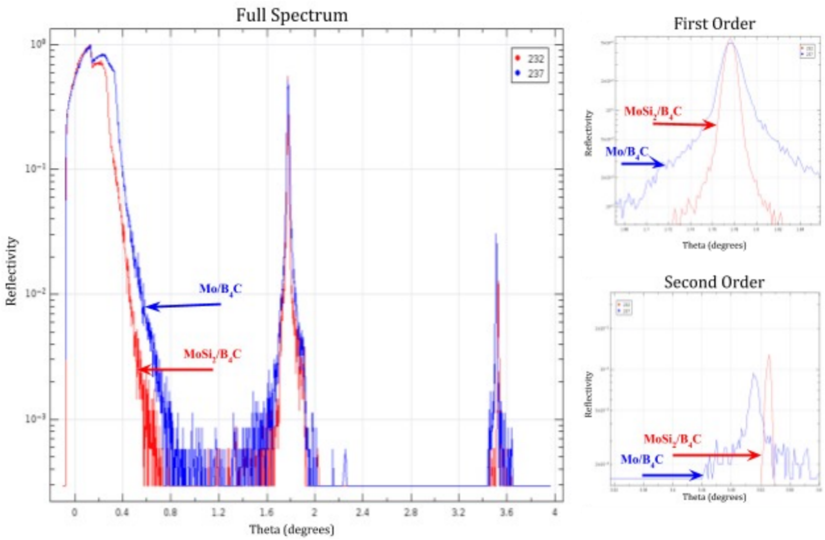

A. Khounsary et al., "A dual-bandwidth multilayer monochromator system," *Proc. SPIE* **10760**, 107600j (2018).

Graded interfaces

Since most interfaces are not sharp, it is important to be able to model a graded interface, where the density, and therefore the index of refraction varies near the interface itself.

Graded interfaces

Since most interfaces are not sharp, it is important to be able to model a graded interface, where the density, and therefore the index of refraction varies near the interface itself.

The reflectivity of this kind of interface can be calculated best in the kinematical limit $(Q > Q_c)$.

Graded interfaces

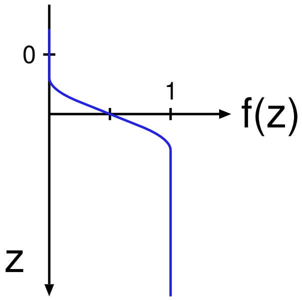

Since most interfaces are not sharp, it is important to be able to model a graded interface, where the density, and therefore the index of refraction varies near the interface itself.

The reflectivity of this kind of interface can be calculated best in the kinematical limit ($Q > Q_c$).

The density profile of the interface can be described by the function $f(z)$ which approaches 1 as $z \to \infty$.

Graded interfaces

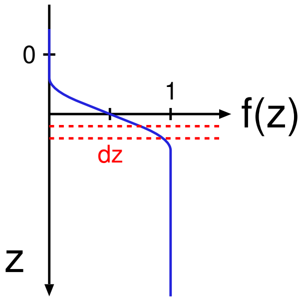

Since most interfaces are not sharp, it is important to be able to model a graded interface, where the density, and therefore the index of refraction varies near the interface itself.

The reflectivity of this kind of interface can be calculated best in the kinematical limit ($Q > Q_c$).

The density profile of the interface can be described by the function $f(z)$ which approaches 1 as $z \to \infty$.

The reflectivity can be computed as the superposition of the reflectivity of a series of infinitesmal slabs of thickness dz at a depth z.

Reflectivity of a graded interface

The differential reflectivity from a slab of thickness dz at depth z is:

Reflectivity of a graded interface

$$\delta r(Q) = -i\frac{Q_c^2}{4Q}f(z)dz$$

The differential reflectivity from a slab of thickness dz at depth z is:

Reflectivity of a graded interface

$$\delta r(Q) = -i\frac{Q_c^2}{4Q}f(z)dz$$

The differential reflectivity from a slab of thickness dz at depth z is:

integrating, to get the entire reflectivity

Reflectivity of a graded interface

The differential reflectivity from a slab of thickness dz at depth z is:

$$\delta r(Q) = -i\frac{Q_c^2}{4Q}f(z)dz$$

integrating, to get the entire reflectivity

$$r(Q) = -i\frac{Q_c^2}{4Q}\int_{-\infty}^{\infty} f(z)e^{iQz}dz$$

Reflectivity of a graded interface

The differential reflectivity from a slab of thickness dz at depth z is:

$$\delta r(Q) = -i\frac{Q_c^2}{4Q} f(z) dz$$

integrating, to get the entire reflectivity

$$r(Q) = -i\frac{Q_c^2}{4Q} \int_{-\infty}^{\infty} f(z) e^{iQz} dz$$

integrating by parts simplifies

Reflectivity of a graded interface

The differential reflectivity from a slab of thickness dz at depth z is:

$$\delta r(Q) = -i\frac{Q_c^2}{4Q}f(z)dz$$

integrating, to get the entire reflectivity

$$r(Q) = -i\frac{Q_c^2}{4Q}\int_{-\infty}^{\infty} f(z)e^{iQz}dz$$

integrating by parts simplifies

$$= i\frac{1}{iQ}\frac{Q_c^2}{4Q}\int_{-\infty}^{\infty} f'(z)e^{iQz}dz$$

Reflectivity of a graded interface

$$\delta r(Q) = -i\frac{Q_c^2}{4Q}f(z)dz$$

$$\begin{aligned} r(Q) &= -i\frac{Q_c^2}{4Q}\int_{-\infty}^{\infty} f(z)e^{iQz}dz \\ &= i\frac{1}{iQ}\frac{Q_c^2}{4Q}\int_{-\infty}^{\infty} f'(z)e^{iQz}dz \\ &= \frac{Q_c^2}{4Q^2}\int_{-\infty}^{\infty} f'(z)e^{iQz}dz \end{aligned}$$

The differential reflectivity from a slab of thickness dz at depth z is:

integrating, to get the entire reflectivity

integrating by parts simplifies

Reflectivity of a graded interface

$$\delta r(Q) = -i\frac{Q_c^2}{4Q}f(z)dz$$

$$r(Q) = -i\frac{Q_c^2}{4Q}\int_{-\infty}^{\infty} f(z)e^{iQz}dz$$

$$= i\frac{1}{iQ}\frac{Q_c^2}{4Q}\int_{-\infty}^{\infty} f'(z)e^{iQz}dz$$

$$= \frac{Q_c^2}{4Q^2}\int_{-\infty}^{\infty} f'(z)e^{iQz}dz$$

The differential reflectivity from a slab of thickness dz at depth z is:

integrating, to get the entire reflectivity

integrating by parts simplifies

the term in front is simply the Fresnel reflectivity for an interface, $r_F(Q)$ when $q \gg 1$

Reflectivity of a graded interface

$$\delta r(Q) = -i\frac{Q_c^2}{4Q}f(z)dz$$

The differential reflectivity from a slab of thickness dz at depth z is:

integrating, to get the entire reflectivity

$$r(Q) = -i\frac{Q_c^2}{4Q}\int_{-\infty}^{\infty} f(z)e^{iQz}dz$$

integrating by parts simplifies

$$= i\frac{1}{iQ}\frac{Q_c^2}{4Q}\int_{-\infty}^{\infty} f'(z)e^{iQz}dz$$

$$= \frac{Q_c^2}{4Q^2}\int_{-\infty}^{\infty} f'(z)e^{iQz}dz$$

the term in front is simply the Fresnel reflectivity for an interface, $r_F(Q)$ when $q \gg 1$, the integral is the Fourier transform of the density gradient, $\phi(Q)$

Reflectivity of a graded interface

The differential reflectivity from a slab of thickness dz at depth z is:

$$\delta r(Q) = -i\frac{Q_c^2}{4Q} f(z)dz$$

integrating, to get the entire reflectivity

$$r(Q) = -i\frac{Q_c^2}{4Q}\int_{-\infty}^{\infty} f(z)e^{iQz}dz$$

integrating by parts simplifies

$$= i\frac{1}{iQ}\frac{Q_c^2}{4Q}\int_{-\infty}^{\infty} f'(z)e^{iQz}dz$$

$$= \frac{Q_c^2}{4Q^2}\int_{-\infty}^{\infty} f'(z)e^{iQz}dz$$

the term in front is simply the Fresnel reflectivity for an interface, $r_F(Q)$ when $q \gg 1$, the integral is the Fourier transform of the density gradient, $\phi(Q)$

Calculating the full reflection coefficient relative to the Fresnel reflection coefficient

$$\frac{R(Q)}{R_F(Q)} = \left|\int_{-\infty}^{\infty}\left(\frac{df}{dz}\right)e^{iQz}dz\right|^2$$

The error function - a specific case

The error function is often chosen as a model for the density gradient

$$f(z) = erf(\frac{z}{\sqrt{2}\sigma}) = \frac{1}{\sqrt{\pi}} \int_0^{z/\sqrt{2}\sigma} e^{-t^2} dt$$

The error function - a specific case

The error function is often chosen as a model for the density gradient

$$f(z) = erf(\frac{z}{\sqrt{2}\sigma}) = \frac{1}{\sqrt{\pi}} \int_0^{z/\sqrt{2}\sigma} e^{-t^2} dt$$

the gradient of the error function is simply a Gaussian

$$\frac{df(z)}{dz} = \frac{d}{dz} erf(\frac{z}{\sqrt{2}\sigma}) = \frac{1}{\sqrt{2\pi\sigma^2}} e^{-\frac{1}{2}\frac{z^2}{\sigma^2}}$$

The error function - a specific case

The error function is often chosen as a model for the density gradient

$$f(z) = erf(\frac{z}{\sqrt{2}\sigma}) = \frac{1}{\sqrt{\pi}} \int_0^{z/\sqrt{2}\sigma} e^{-t^2} dt$$

the gradient of the error function is simply a Gaussian

$$\frac{df(z)}{dz} = \frac{d}{dz} erf(\frac{z}{\sqrt{2}\sigma}) = \frac{1}{\sqrt{2\pi\sigma^2}} e^{-\frac{1}{2}\frac{z^2}{\sigma^2}}$$

whose Fourier transform is also a Gaussian, which when squared to obtain the reflection coefficient, gives.

$$R(Q) = R_F(Q) e^{-Q^2\sigma^2}$$

The error function - a specific case

The error function is often chosen as a model for the density gradient

$$f(z) = erf(\frac{z}{\sqrt{2}\sigma}) = \frac{1}{\sqrt{\pi}} \int_0^{z/\sqrt{2}\sigma} e^{-t^2} dt$$

the gradient of the error function is simply a Gaussian

$$\frac{df(z)}{dz} = \frac{d}{dz} erf(\frac{z}{\sqrt{2}\sigma}) = \frac{1}{\sqrt{2\pi\sigma^2}} e^{-\frac{1}{2}\frac{z^2}{\sigma^2}}$$

whose Fourier transform is also a Gaussian, which when squared to obtain the reflection coefficient, gives. Or more accurately.

$$R(Q) = R_F(Q) e^{-Q^2\sigma^2} = R_F(Q) e^{-QQ'\sigma^2}$$

The error function - a specific case

The error function is often chosen as a model for the density gradient

$$f(z) = erf(\frac{z}{\sqrt{2}\sigma}) = \frac{1}{\sqrt{\pi}} \int_0^{z/\sqrt{2}\sigma} e^{-t^2} dt$$

the gradient of the error function is simply a Gaussian

$$\frac{df(z)}{dz} = \frac{d}{dz} erf(\frac{z}{\sqrt{2}\sigma}) = \frac{1}{\sqrt{2\pi\sigma^2}} e^{-\frac{1}{2}\frac{z^2}{\sigma^2}}$$

whose Fourier transform is also a Gaussian, which when squared to obtain the reflection coefficient, gives. Or more accurately.

$$R(Q) = R_F(Q) e^{-Q^2\sigma^2} = R_F(Q) e^{-QQ'\sigma^2}$$

$$Q = k \sin\theta, \qquad Q' = k' \sin\theta'$$

Rough surfaces

When a surface or interface is not perfectly smooth but has some roughness the reflectivity is no longer simply specular but has a non-zero diffuse component which we must include in the model.

Rough surfaces

When a surface or interface is not perfectly smooth but has some roughness the reflectivity is no longer simply specular but has a non-zero diffuse component which we must include in the model.

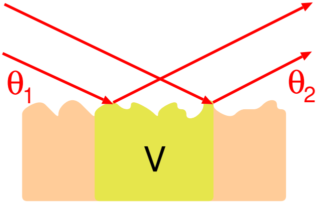

Rough surfaces

When a surface or interface is not perfectly smooth but has some roughness the reflectivity is no longer simply specular but has a non-zero diffuse component which we must include in the model.

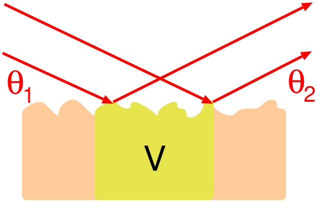

The incident and scattered angles are no longer the same, the x-rays illuminate the volume V.

Rough surfaces

When a surface or interface is not perfectly smooth but has some roughness the reflectivity is no longer simply specular but has a non-zero diffuse component which we must include in the model.

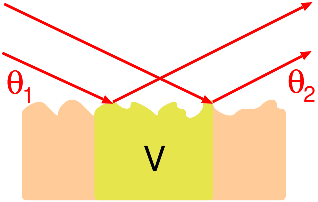

The incident and scattered angles are no longer the same, the x-rays illuminate the volume V. The scattering from the entire, illuminated volume is given by

Rough surfaces

When a surface or interface is not perfectly smooth but has some roughness the reflectivity is no longer simply specular but has a non-zero diffuse component which we must include in the model.

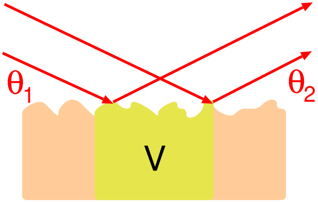

$$r_V = -r_0 \int_V (\rho d\vec{r}) e^{i\vec{Q}\cdot\vec{r}}$$

The incident and scattered angles are no longer the same, the x-rays illuminate the volume V. The scattering from the entire, illuminated volume is given by

Rough surfaces

When a surface or interface is not perfectly smooth but has some roughness the reflectivity is no longer simply specular but has a non-zero diffuse component which we must include in the model.

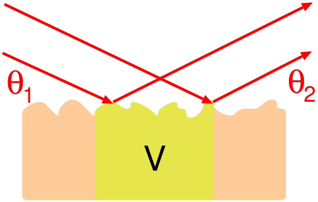

$$r_V = -r_0 \int_V (\rho d\vec{r}) e^{i\vec{Q}\cdot\vec{r}}$$

The incident and scattered angles are no longer the same, the x-rays illuminate the volume V. The scattering from the entire, illuminated volume is given by using Gauss' theorem.

Rough surfaces

When a surface or interface is not perfectly smooth but has some roughness the reflectivity is no longer simply specular but has a non-zero diffuse component which we must include in the model.

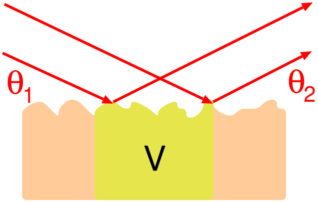

$$r_V = -r_0 \int_V (\rho d\vec{r}) e^{i\vec{Q}\cdot\vec{r}}$$

$$\int_V \left(\vec{\nabla}\cdot\vec{C}\right) d\vec{r} = \int_S \vec{C}\cdot d\vec{S}$$

The incident and scattered angles are no longer the same, the x-rays illuminate the volume V. The scattering from the entire, illuminated volume is given by using Gauss' theorem.

Conversion to surface integral

$$\int_V \left(\vec{\nabla} \cdot \vec{C}\right) d\vec{r} = \int_S \vec{C} \cdot d\vec{S}$$

$$r_V = -r_0 \rho \int_V e^{i\vec{Q}\cdot\vec{r}} d\vec{r}$$

Conversion to surface integral

$$\int_V \left(\vec{\nabla} \cdot \vec{C}\right) d\vec{r} = \int_S \vec{C} \cdot d\vec{S}$$

$$r_V = -r_0 \rho \int_V e^{i\vec{Q}\cdot\vec{r}} d\vec{r}$$

Taking

$$\vec{C} = \hat{z}\frac{e^{i\vec{Q}\cdot\vec{r}}}{iQ_z}$$

Conversion to surface integral

$$\int_V \left(\vec{\nabla} \cdot \vec{C}\right) d\vec{r} = \int_S \vec{C} \cdot d\vec{S}$$

$$r_V = -r_0 \rho \int_V e^{i\vec{Q}\cdot\vec{r}} d\vec{r}$$

Taking

$$\vec{C} = \hat{z} \frac{e^{i\vec{Q}\cdot\vec{r}}}{iQ_z}$$

We have

$$\vec{\nabla} \cdot \vec{C} = \frac{e^{i\vec{Q}\cdot\vec{r}}}{iQ_z} iQ_z$$

Conversion to surface integral

$$\int_V \left(\vec{\nabla} \cdot \vec{C}\right) d\vec{r} = \int_S \vec{C} \cdot d\vec{S}$$

$$r_V = -r_0 \rho \int_V e^{i\vec{Q}\cdot\vec{r}} d\vec{r}$$

Taking

$$\vec{C} = \hat{z}\frac{e^{i\vec{Q}\cdot\vec{r}}}{iQ_z}$$

We have

$$\vec{\nabla} \cdot \vec{C} = \frac{e^{i\vec{Q}\cdot\vec{r}}}{iQ_z} iQ_z = e^{i\vec{Q}\cdot\vec{r}}$$

Conversion to surface integral

$$\int_V \left(\vec{\nabla} \cdot \vec{C}\right) d\vec{r} = \int_S \vec{C} \cdot d\vec{S}$$

Taking

$$\vec{C} = \hat{z}\frac{e^{i\vec{Q}\cdot\vec{r}}}{iQ_z}$$

We have

$$\vec{\nabla} \cdot \vec{C} = \frac{e^{i\vec{Q}\cdot\vec{r}}}{iQ_z} iQ_z = e^{i\vec{Q}\cdot\vec{r}}$$

$$\begin{aligned} r_V &= -r_0\rho \int_V e^{i\vec{Q}\cdot\vec{r}} d\vec{r} \\ &= -r_0\rho \int_V \vec{\nabla} \cdot \left(\hat{z}\frac{e^{i\vec{Q}\cdot\vec{r}}}{iQ_z}\right) \cdot d\vec{r} \end{aligned}$$

Conversion to surface integral

$$\int_V \left(\vec{\nabla} \cdot \vec{C}\right) d\vec{r} = \int_S \vec{C} \cdot d\vec{S}$$

Taking

$$\vec{C} = \hat{z}\frac{e^{i\vec{Q}\cdot\vec{r}}}{iQ_z}$$

We have

$$\vec{\nabla} \cdot \vec{C} = \frac{e^{i\vec{Q}\cdot\vec{r}}}{iQ_z} iQ_z = e^{i\vec{Q}\cdot\vec{r}}$$

$$\begin{aligned} r_V &= -r_0\rho \int_V e^{i\vec{Q}\cdot\vec{r}} d\vec{r} \\ &= -r_0\rho \int_V \vec{\nabla} \cdot \left(\hat{z}\frac{e^{i\vec{Q}\cdot\vec{r}}}{iQ_z}\right) \cdot d\vec{r} \end{aligned}$$

$$r_S = -r_0\rho \int_S \left(\hat{z}\frac{e^{i\vec{Q}\cdot\vec{r}}}{iQ_z}\right) \cdot d\vec{S}$$

Conversion to surface integral

$$\int_V \left(\vec{\nabla} \cdot \vec{C}\right) d\vec{r} = \int_S \vec{C} \cdot d\vec{S}$$

Taking

$$\vec{C} = \hat{z}\frac{e^{i\vec{Q}\cdot\vec{r}}}{iQ_z}$$

We have

$$\vec{\nabla} \cdot \vec{C} = \frac{e^{i\vec{Q}\cdot\vec{r}}}{iQ_z} iQ_z = e^{i\vec{Q}\cdot\vec{r}}$$

$$r_V = -r_0\rho \int_V e^{i\vec{Q}\cdot\vec{r}} d\vec{r}$$

$$= -r_0\rho \int_V \vec{\nabla} \cdot \left(\hat{z}\frac{e^{i\vec{Q}\cdot\vec{r}}}{iQ_z}\right) \cdot d\vec{r}$$

$$r_S = -r_0\rho \int_S \left(\hat{z}\frac{e^{i\vec{Q}\cdot\vec{r}}}{iQ_z}\right) \cdot d\vec{S}$$

$$r_S = -r_0\rho \frac{1}{iQ_z} \int_S e^{i\vec{Q}\cdot\vec{r}} dxdy$$

Evaluation of surface integral

The side surfaces of the volume do not contribute to this integral as they are along the $\hat{z}$ direction, and we can also choose the thickness of the slab sufficiently large such that the lower surface will not contribute.

Evaluation of surface integral

The side surfaces of the volume do not contribute to this integral as they are along the $\hat{z}$ direction, and we can also choose the thickness of the slab sufficiently large such that the lower surface will not contribute.

Thus, the integral need only be evaluated over the top, rough surface whose variation we characterize by the function $h(x, y)$

Evaluation of surface integral

The side surfaces of the volume do not contribute to this integral as they are along the $\hat{z}$ direction, and we can also choose the thickness of the slab sufficiently large such that the lower surface will not contribute.

Thus, the integral need only be evaluated over the top, rough surface whose variation we characterize by the function $h(x, y)$

$$\vec{Q} \cdot \vec{r} = Q_z h(x, y) + Q_x x + Q_y y$$

Evaluation of surface integral

The side surfaces of the volume do not contribute to this integral as they are along the $\hat{z}$ direction, and we can also choose the thickness of the slab sufficiently large such that the lower surface will not contribute.

Thus, the integral need only be evaluated over the top, rough surface whose variation we characterize by the function $h(x, y)$

$$\vec{Q} \cdot \vec{r} = Q_z h(x, y) + Q_x x + Q_y y$$

$$r_S = -\frac{r_0 \rho}{iQ_z} \int_S e^{iQ_z h(x,y)} e^{i(Q_x x + Q_y y)} dxdy$$

Evaluation of surface integral

The side surfaces of the volume do not contribute to this integral as they are along the $\hat{z}$ direction, and we can also choose the thickness of the slab sufficiently large such that the lower surface will not contribute.

Thus, the integral need only be evaluated over the top, rough surface whose variation we characterize by the function $h(x,y)$

$$\vec{Q} \cdot \vec{r} = Q_z h(x,y) + Q_x x + Q_y y$$

$$r_S = -\frac{r_0 \rho}{iQ_z} \int_S e^{iQ_z h(x,y)} e^{i(Q_x x + Q_y y)} dxdy$$

The actual scattering cross section is the square of this integral

$$\frac{d\sigma}{d\Omega} = \left(\frac{r_0 \rho}{Q_z} \right)^2 \int_S \int_{S'} e^{iQ_z(h(x,y) - h(x',y'))} e^{iQ_x(x-x')} e^{iQ_y(y-y')} dxdydx'dy'$$

Scattering cross section

If we assume that $h(x, y) - h(x', y')$ depends only on the relative difference in position, $x - x'$ and $y - y'$ the four dimensional integral collapses to the product of two two dimensional integrals

Scattering cross section

If we assume that $h(x, y) - h(x', y')$ depends only on the relative difference in position, $x - x'$ and $y - y'$ the four dimensional integral collapses to the product of two two dimensional integrals

$$\left(\frac{d\sigma}{d\Omega}\right) = \left(\frac{r_0\rho}{Q_z}\right)^2 \int_{S'} dx'dy' \int_S \left\langle e^{iQ_z(h(0,0)-h(x,y))} \right\rangle e^{iQ_x x} e^{iQ_y y} dxdy$$

Scattering cross section

If we assume that $h(x, y) - h(x', y')$ depends only on the relative difference in position, $x - x'$ and $y - y'$ the four dimensional integral collapses to the product of two two dimensional integrals

$$\left(\frac{d\sigma}{d\Omega}\right) = \left(\frac{r_0\rho}{Q_z}\right)^2 \int_{S'} dx'dy' \int_S \left\langle e^{iQ_z(h(0,0)-h(x,y))} \right\rangle e^{iQ_x x} e^{iQ_y y} dxdy$$

$$= \left(\frac{r_0\rho}{Q_z}\right)^2 \frac{A_0}{\sin\theta_1} \int \left\langle e^{iQ_z(h(0,0)-h(x,y))} \right\rangle e^{iQ_x x} e^{iQ_y y} dxdy$$

Scattering cross section

If we assume that $h(x, y) - h(x', y')$ depends only on the relative difference in position, $x - x'$ and $y - y'$ the four dimensional integral collapses to the product of two two dimensional integrals

$$\left(\frac{d\sigma}{d\Omega}\right) = \left(\frac{r_0\rho}{Q_z}\right)^2 \int_{S'} dx'dy' \int_S \left\langle e^{iQ_z(h(0,0)-h(x,y))}\right\rangle e^{iQ_x x} e^{iQ_y y} dxdy$$

$$= \left(\frac{r_0\rho}{Q_z}\right)^2 \frac{A_0}{\sin\theta_1} \int \left\langle e^{iQ_z(h(0,0)-h(x,y))}\right\rangle e^{iQ_x x} e^{iQ_y y} dxdy$$

where $A_0/\sin\theta_1$ is just the illuminated surface area

Scattering cross section

If we assume that $h(x,y) - h(x',y')$ depends only on the relative difference in position, $x - x'$ and $y - y'$ the four dimensional integral collapses to the product of two two dimensional integrals

$$\left(\frac{d\sigma}{d\Omega}\right) = \left(\frac{r_0\rho}{Q_z}\right)^2 \int_{S'} dx'dy' \int_S \left\langle e^{iQ_z(h(0,0)-h(x,y))} \right\rangle e^{iQ_x x} e^{iQ_y y} dxdy$$

$$= \left(\frac{r_0\rho}{Q_z}\right)^2 \frac{A_0}{\sin\theta_1} \int \left\langle e^{iQ_z(h(0,0)-h(x,y))} \right\rangle e^{iQ_x x} e^{iQ_y y} dxdy$$

where $A_0/\sin\theta_1$ is just the illuminated surface area and the term in the angled brackets is an ensemble average over all possible choices of the origin within the illuminated area.

Scattering cross section

If we assume that $h(x, y) - h(x', y')$ depends only on the relative difference in position, $x - x'$ and $y - y'$ the four dimensional integral collapses to the product of two two dimensional integrals

$$\left(\frac{d\sigma}{d\Omega}\right) = \left(\frac{r_0\rho}{Q_z}\right)^2 \int_{S'} dx'dy' \int_S \left\langle e^{iQ_z(h(0,0)-h(x,y))}\right\rangle e^{iQ_x x} e^{iQ_y y} dxdy$$

$$= \left(\frac{r_0\rho}{Q_z}\right)^2 \frac{A_0}{\sin\theta_1} \int \left\langle e^{iQ_z(h(0,0)-h(x,y))}\right\rangle e^{iQ_x x} e^{iQ_y y} dxdy$$

where $A_0/\sin\theta_1$ is just the illuminated surface area and the term in the angled brackets is an ensemble average over all possible choices of the origin within the illuminated area.

Finally, it is assumed that the statistics of the height variation are Gaussian and

$$\left(\frac{d\sigma}{d\Omega}\right) = \left(\frac{r_0\rho}{Q_z}\right)^2 \frac{A_0}{\sin\theta_1} \int e^{-Q_z^2\left\langle [h(0,0)-h(x,y)]^2\right\rangle/2} e^{iQ_x x} e^{iQ_y y} dxdy$$

Limiting Case - Flat surface

Define a function $g(x, y) = \left\langle [h(0,0) - h(x,y)]^2 \right\rangle$ which can be modeled in various ways.

Limiting Case - Flat surface

Define a function $g(x, y) = \left\langle [h(0,0) - h(x,y)]^2 \right\rangle$ which can be modeled in various ways.

For a perfectly flat surface, $h(x, y) = 0$ for all x and y.

Limiting Case - Flat surface

Define a function $g(x,y) = \left\langle [h(0,0) - h(x,y)]^2 \right\rangle$ which can be modeled in various ways.

For a perfectly flat surface, $h(x,y) = 0$ for all x and y.

$$\left(\frac{d\sigma}{d\Omega}\right) = \left(\frac{r_0\rho}{Q_z}\right)^2 \frac{A_0}{\sin\theta_1} \int e^{iQ_x x} e^{iQ_y y} dxdy$$

Limiting Case - Flat surface

Define a function $g(x,y) = \left\langle [h(0,0) - h(x,y)]^2 \right\rangle$ which can be modeled in various ways.

For a perfectly flat surface, $h(x,y) = 0$ for all x and y.

by the definition of a delta function

$$2\pi\delta(q) = \int e^{iqx} dx$$

$$\left(\frac{d\sigma}{d\Omega}\right) = \left(\frac{r_0\rho}{Q_z}\right)^2 \frac{A_0}{\sin\theta_1} \int e^{iQ_x x} e^{iQ_y y} dx dy$$

Limiting Case - Flat surface

Define a function $g(x, y) = \left\langle [h(0,0) - h(x,y)]^2 \right\rangle$ which can be modeled in various ways.

For a perfectly flat surface, $h(x, y) = 0$ for all x and y.

by the definition of a delta function

$$2\pi\delta(q) = \int e^{iqx} dx$$

$$\left(\frac{d\sigma}{d\Omega}\right) = \left(\frac{r_0 \rho}{Q_z}\right)^2 \frac{A_0}{\sin\theta_1} \int e^{iQ_x x} e^{iQ_y y} dx dy$$
$$= \left(\frac{r_0 \rho}{Q_z}\right)^2 \frac{A_0}{\sin\theta_1} \delta(Q_x)\delta(Q_y)$$

Limiting Case - Flat surface

Define a function $g(x, y) = \left\langle [h(0,0) - h(x,y)]^2 \right\rangle$ which can be modeled in various ways.

For a perfectly flat surface, $h(x, y) = 0$ for all x and y.

by the definition of a delta function

$$2\pi\delta(q) = \int e^{iqx} dx$$

the expression for the scattered intensity in terms of the momentum transfer wave vectors is

$$\left(\frac{d\sigma}{d\Omega}\right) = \left(\frac{r_0\rho}{Q_z}\right)^2 \frac{A_0}{\sin\theta_1} \int e^{iQ_x x} e^{iQ_y y} dxdy$$

$$= \left(\frac{r_0\rho}{Q_z}\right)^2 \frac{A_0}{\sin\theta_1} \delta(Q_x)\delta(Q_y)$$

Limiting Case - Flat surface

Define a function $g(x, y) = \left\langle [h(0,0) - h(x,y)]^2 \right\rangle$ which can be modeled in various ways.

For a perfectly flat surface, $h(x, y) = 0$ for all x and y.

by the definition of a delta function

$$2\pi\delta(q) = \int e^{iqx} dx$$

$$\left(\frac{d\sigma}{d\Omega}\right) = \left(\frac{r_0\rho}{Q_z}\right)^2 \frac{A_0}{\sin\theta_1} \int e^{iQ_x x} e^{iQ_y y} dxdy$$
$$= \left(\frac{r_0\rho}{Q_z}\right)^2 \frac{A_0}{\sin\theta_1} \delta(Q_x)\delta(Q_y)$$

the expression for the scattered intensity in terms of the momentum transfer wave vectors is

$$I_{sc} = \left(\frac{I_0}{A_0}\right) \left(\frac{d\sigma}{d\Omega}\right) \frac{\Delta Q_x \Delta Q_y}{k^2 \sin\theta_2}$$

Limiting Case - Flat surface

Define a function $g(x,y) = \left\langle [h(0,0) - h(x,y)]^2 \right\rangle$ which can be modeled in various ways.

For a perfectly flat surface, $h(x,y) = 0$ for all x and y.

by the definition of a delta function

$$2\pi\delta(q) = \int e^{iqx} dx$$

$$\left(\frac{d\sigma}{d\Omega}\right) = \left(\frac{r_0\rho}{Q_z}\right)^2 \frac{A_0}{\sin\theta_1} \int e^{iQ_x x} e^{iQ_y y} dxdy$$
$$= \left(\frac{r_0\rho}{Q_z}\right)^2 \frac{A_0}{\sin\theta_1} \delta(Q_x)\delta(Q_y)$$

the expression for the scattered intensity in terms of the momentum transfer wave vectors is

$$I_{sc} = \left(\frac{I_0}{A_0}\right)\left(\frac{d\sigma}{d\Omega}\right)\frac{\Delta Q_x \Delta Q_y}{k^2 \sin\theta_2}$$

$$R(Q_z) = \frac{I_{sc}}{I_0} = \left(\frac{Q_c^2/8}{Q_z}\right)^2 \left(\frac{1}{Q_z/2}\right)^2 = \left(\frac{Q_c}{2Q_z}\right)^4$$

Uncorrelated surfaces

For a totally uncorrelated surface, $h(x, y)$ is independent from $h(x', y')$ and

Uncorrelated surfaces

For a totally uncorrelated surface, $h(x, y)$ is independent from $h(x', y')$ and

$$\left\langle [h(0,0) - h(x,y)]^2 \right\rangle = \langle h(0,0) \rangle^2 - 2 \langle h(0,0) \rangle \langle h(x,y) \rangle + \langle h(x,y) \rangle^2$$

Uncorrelated surfaces

For a totally uncorrelated surface, $h(x, y)$ is independent from $h(x', y')$ and

$$\left\langle [h(0,0) - h(x,y)]^2 \right\rangle = \langle h(0,0)\rangle^2 - 2\,\langle h(0,0)\rangle\,\langle h(x,y)\rangle + \langle h(x,y)\rangle^2$$
$$= 2\left\langle h^2 \right\rangle$$

Uncorrelated surfaces

For a totally uncorrelated surface, $h(x, y)$ is independent from $h(x', y')$ and

$$\left\langle [h(0,0) - h(x,y)]^2 \right\rangle = \langle h(0,0)\rangle^2 - 2\,\langle h(0,0)\rangle\,\langle h(x,y)\rangle + \langle h(x,y)\rangle^2$$
$$= 2\left\langle h^2 \right\rangle$$

This quantity is simply related to the rms roughness, σ by $\sigma^2 = \left\langle h^2 \right\rangle$ and the cross-section is given by

$$\left(\frac{d\sigma}{d\Omega}\right) =$$

Uncorrelated surfaces

For a totally uncorrelated surface, $h(x,y)$ is independent from $h(x',y')$ and

$$\left\langle [h(0,0)-h(x,y)]^2 \right\rangle = \langle h(0,0)\rangle^2 - 2\,\langle h(0,0)\rangle\,\langle h(x,y)\rangle + \langle h(x,y)\rangle^2$$
$$= 2\left\langle h^2 \right\rangle$$

This quantity is simply related to the rms roughness, σ by $\sigma^2 = \left\langle h^2 \right\rangle$ and the cross-section is given by

$$\left(\frac{d\sigma}{d\Omega}\right) = \left(\frac{r_0\rho}{Q_z}\right)^2 \frac{A_0}{\sin\theta_1} \int e^{-Q_z^2\left\langle h^2\right\rangle/2} e^{iQ_x x} e^{iQ_y y}\,dxdy$$

Uncorrelated surfaces

For a totally uncorrelated surface, $h(x, y)$ is independent from $h(x', y')$ and

$$\left\langle [h(0,0) - h(x,y)]^2 \right\rangle = \langle h(0,0) \rangle^2 - 2 \langle h(0,0) \rangle \langle h(x,y) \rangle + \langle h(x,y) \rangle^2$$
$$= 2 \left\langle h^2 \right\rangle$$

This quantity is simply related to the rms roughness, σ by $\sigma^2 = \left\langle h^2 \right\rangle$ and the cross-section is given by

$$\left(\frac{d\sigma}{d\Omega}\right) = \left(\frac{r_0 \rho}{Q_z}\right)^2 \frac{A_0}{\sin\theta_1} \int e^{-Q_z^2 \left\langle h^2 \right\rangle / 2} e^{iQ_x x} e^{iQ_y y} dx dy$$
$$= \left(\frac{r_0 \rho}{Q_z}\right)^2 \frac{A_0}{\sin\theta_1} e^{-Q_z^2 \sigma^2} \int e^{iQ_x x} e^{iQ_y y} dx dy$$

Uncorrelated surfaces

For a totally uncorrelated surface, $h(x,y)$ is independent from $h(x',y')$ and

$$\left\langle [h(0,0)-h(x,y)]^2 \right\rangle = \langle h(0,0)\rangle^2 - 2\,\langle h(0,0)\rangle\,\langle h(x,y)\rangle + \langle h(x,y)\rangle^2$$
$$= 2\left\langle h^2 \right\rangle$$

This quantity is simply related to the rms roughness, σ by $\sigma^2 = \left\langle h^2 \right\rangle$ and the cross-section is given by

$$\left(\frac{d\sigma}{d\Omega}\right) = \left(\frac{r_0\rho}{Q_z}\right)^2 \frac{A_0}{\sin\theta_1} \int e^{-Q_z^2\left\langle h^2\right\rangle/2} e^{iQ_x x} e^{iQ_y y} dxdy$$
$$= \left(\frac{r_0\rho}{Q_z}\right)^2 \frac{A_0}{\sin\theta_1} e^{-Q_z^2\sigma^2} \int e^{iQ_x x} e^{iQ_y y} dxdy$$

Which, apart from the term containing σ is simply the Fresnel cross-section for a flat surface

Uncorrelated surfaces

For a totally uncorrelated surface, $h(x,y)$ is independent from $h(x',y')$ and

$$\left\langle [h(0,0) - h(x,y)]^2 \right\rangle = \langle h(0,0)\rangle^2 - 2\,\langle h(0,0)\rangle\,\langle h(x,y)\rangle + \langle h(x,y)\rangle^2$$
$$= 2\left\langle h^2 \right\rangle$$

This quantity is simply related to the rms roughness, σ by $\sigma^2 = \left\langle h^2 \right\rangle$ and the cross-section is given by

$$\left(\frac{d\sigma}{d\Omega}\right) = \left(\frac{r_0\rho}{Q_z}\right)^2 \frac{A_0}{\sin\theta_1} \int e^{-Q_z^2\left\langle h^2\right\rangle/2} e^{iQ_x x} e^{iQ_y y}\,dxdy$$
$$= \left(\frac{r_0\rho}{Q_z}\right)^2 \frac{A_0}{\sin\theta_1} e^{-Q_z^2\sigma^2} \int e^{iQ_x x} e^{iQ_y y}\,dxdy$$

Which, apart from the term containing σ is simply the Fresnel cross-section for a flat surface

$$\left(\frac{d\sigma}{d\Omega}\right) = \left(\frac{d\sigma}{d\Omega}\right)_{Fresnel} e^{-Q_z^2\sigma^2}$$

Surface roughness effect

$$\left(\frac{d\sigma}{d\Omega}\right) = \left(\frac{d\sigma}{d\Omega}\right)_{Fresnel} e^{-Q_z^2\sigma^2}$$

Surface roughness effect

$$\left(\frac{d\sigma}{d\Omega}\right) = \left(\frac{d\sigma}{d\Omega}\right)_{Fresnel} e^{-Q_z^2\sigma^2}$$

for a perfectly flat surface, we get the Fresnel reflectivity derived for a thin slab

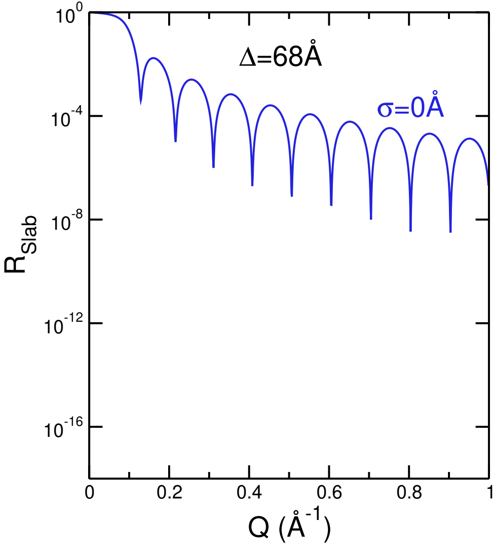

Surface roughness effect

$$\left(\frac{d\sigma}{d\Omega}\right) = \left(\frac{d\sigma}{d\Omega}\right)_{Fresnel} e^{-Q_z^2\sigma^2}$$

for a perfectly flat surface, we get the Fresnel reflectivity derived for a thin slab

for an uncorrelated rough surface, the reflectivity is reduced by an exponential factor controlled by the rms surface roughness σ

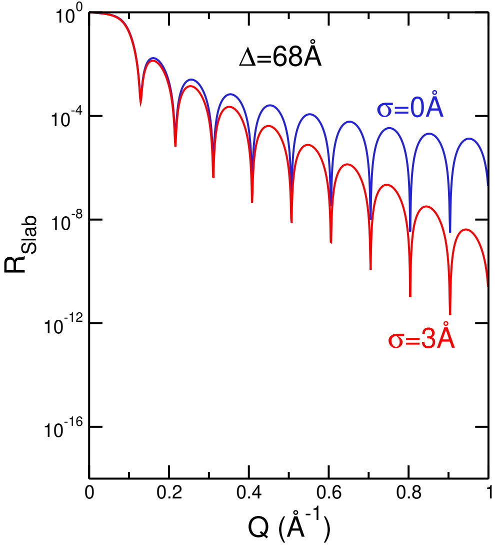

Surface roughness effect

$$\left(\frac{d\sigma}{d\Omega}\right) = \left(\frac{d\sigma}{d\Omega}\right)_{Fresnel} e^{-Q_z^2\sigma^2}$$

for a perfectly flat surface, we get the Fresnel reflectivity derived for a thin slab

for an uncorrelated rough surface, the reflectivity is reduced by an exponential factor controlled by the rms surface roughness σ

this leads to a rapid drop in reflectivity as the surface roughness increases

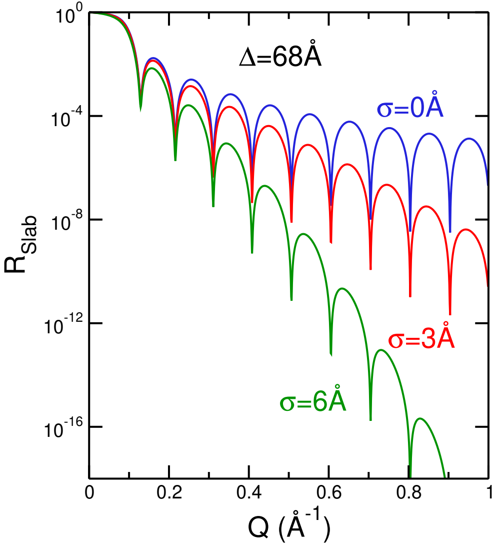

Correlated surfaces

Assume that height fluctuations are isotropically correlated in the x-y plane. Therefore, $g(x, y) = g(r) = g(\sqrt{x^2 + y^2})$.

Correlated surfaces

Assume that height fluctuations are isotropically correlated in the x-y plane. Therefore, $g(x, y) = g(r) = g(\sqrt{x^2 + y^2})$.

In the limit that the correlations are unbounded as $r \to \infty$, $g(x, y)$ is given by

$$g(x, y) = \mathcal{A} r^{2h}$$

where h is a fractal parameter which defines the shape of the surface.

Correlated surfaces

Assume that height fluctuations are isotropically correlated in the x-y plane. Therefore, $g(x, y) = g(r) = g(\sqrt{x^2 + y^2})$.

In the limit that the correlations are unbounded as $r \to \infty$, $g(x, y)$ is given by

$$g(x, y) = \mathcal{A} r^{2h}$$

where h is a fractal parameter which defines the shape of the surface.

jagged surface for $h \ll 1$

Correlated surfaces

Assume that height fluctuations are isotropically correlated in the x-y plane. Therefore, $g(x, y) = g(r) = g(\sqrt{x^2 + y^2})$.

In the limit that the correlations are unbounded as $r \to \infty$, $g(x, y)$ is given by

$$g(x, y) = \mathcal{A} r^{2h}$$

where h is a fractal parameter which defines the shape of the surface.

jagged surface for $h \ll 1$ smoother surface for $h \to 1$

Correlated surfaces

Assume that height fluctuations are isotropically correlated in the x-y plane. Therefore, $g(x, y) = g(r) = g(\sqrt{x^2 + y^2})$.

In the limit that the correlations are unbounded as $r \to \infty$, $g(x, y)$ is given by

$$g(x, y) = \mathcal{A} r^{2h}$$

where h is a fractal parameter which defines the shape of the surface.

jagged surface for $h \ll 1$ smoother surface for $h \to 1$

If the resolution in the y direction is very broad (typical for a synchrotron), we can eliminate the y-integral and have

Correlated surfaces

Assume that height fluctuations are isotropically correlated in the x-y plane. Therefore, $g(x, y) = g(r) = g(\sqrt{x^2 + y^2})$.

In the limit that the correlations are unbounded as $r \to \infty$, $g(x, y)$ is given by

$$g(x, y) = \mathcal{A} r^{2h}$$

where h is a fractal parameter which defines the shape of the surface.

jagged surface for $h \ll 1$ smoother surface for $h \to 1$

If the resolution in the y direction is very broad (typical for a synchrotron), we can eliminate the y-integral and have

$$\left(\frac{d\sigma}{d\Omega}\right) = \left(\frac{r_0 \rho}{Q_z}\right)^2 \frac{A_0}{\sin\theta_1} \int e^{-\mathcal{A} Q_z^2 |x|^{2h}/2} \cos(Q_x x) dx$$

Unbounded correlations - limiting cases

This integral can be evaluated in closed form for two special cases, both having a broad diffuse scattering and no specular peak.

Unbounded correlations - limiting cases

This integral can be evaluated in closed form for two special cases, both having a broad diffuse scattering and no specular peak.

$h = 1/2$

$$\left(\frac{d\sigma}{d\Omega}\right) = \left(\frac{A_0 r_0^2 \rho^2}{2\sin\theta_1}\right) \frac{\mathcal{A}}{(Q_x^2 + (\mathcal{A}/2)^2 Q_z^4)}$$

Unbounded correlations - limiting cases

This integral can be evaluated in closed form for two special cases, both having a broad diffuse scattering and no specular peak.

$h = 1/2$

$$\left(\frac{d\sigma}{d\Omega}\right) = \left(\frac{A_0 r_0^2 \rho^2}{2\sin\theta_1}\right) \frac{\mathcal{A}}{(Q_x^2 + (\mathcal{A}/2)^2 Q_z^4)}$$

Lorentzian with half-width $\mathcal{A}Q_z^2/2$

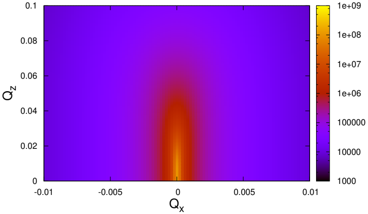

Unbounded correlations - limiting cases

This integral can be evaluated in closed form for two special cases, both having a broad diffuse scattering and no specular peak.

$h = 1/2$

$$\left(\frac{d\sigma}{d\Omega}\right) = \left(\frac{A_0 r_0^2 \rho^2}{2\sin\theta_1}\right) \frac{\mathcal{A}}{(Q_x^2 + (\mathcal{A}/2)^2 Q_z^4)}$$

Lorentzian with half-width $\mathcal{A}Q_z^2/2$

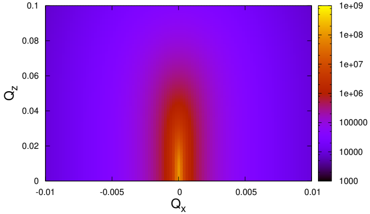

$h = 1$

$$\left(\frac{d\sigma}{d\Omega}\right) = \left(\frac{2\sqrt{\pi} A_0 r_0^2 \rho^2}{2\sin\theta_1}\right) \frac{1}{Q_z^4} e^{-\frac{1}{2}\left(\frac{Q_x^2}{\mathcal{A}Q_z^2}\right)}$$

Unbounded correlations - limiting cases

This integral can be evaluated in closed form for two special cases, both having a broad diffuse scattering and no specular peak.

$h = 1/2$

$$\left(\frac{d\sigma}{d\Omega}\right) = \left(\frac{A_0 r_0^2 \rho^2}{2\sin\theta_1}\right) \frac{\mathcal{A}}{(Q_x^2 + (\mathcal{A}/2)^2 Q_z^4)}$$

Lorentzian with half-width $\mathcal{A}Q_z^2/2$

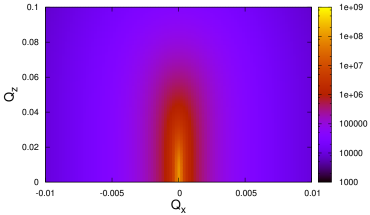

$h = 1$

$$\left(\frac{d\sigma}{d\Omega}\right) = \left(\frac{2\sqrt{\pi} A_0 r_0^2 \rho^2}{2\sin\theta_1}\right) \frac{1}{Q_z^4} e^{-\frac{1}{2}\left(\frac{Q_x^2}{\mathcal{A}Q_z^2}\right)}$$

Unbounded correlations - limiting cases

This integral can be evaluated in closed form for two special cases, both having a broad diffuse scattering and no specular peak.

$h = 1/2$

$$\left(\frac{d\sigma}{d\Omega}\right) = \left(\frac{A_0 r_0^2 \rho^2}{2 \sin\theta_1}\right) \frac{\mathcal{A}}{(Q_x^2 + (\mathcal{A}/2)^2 Q_z^4)}$$

Lorentzian with half-width $\mathcal{A}Q_z^2/2$

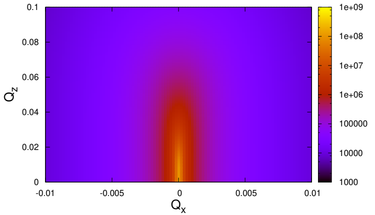

$h = 1$

$$\left(\frac{d\sigma}{d\Omega}\right) = \left(\frac{2\sqrt{\pi} A_0 r_0^2 \rho^2}{2 \sin\theta_1}\right) \frac{1}{Q_z^4} e^{-\frac{1}{2}\left(\frac{Q_x^2}{\mathcal{A}Q_z^2}\right)}$$

Gaussian with variance $\mathcal{A}Q_z^2$

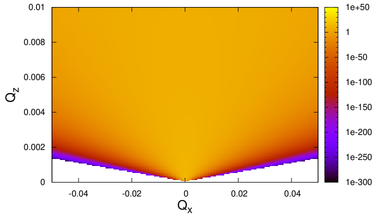

Bounded correlations

If the correlations remain bounded as $r \rightarrow \infty$

Bounded correlations

If the correlations remain bounded as $r \to \infty$

$$g(x, y) = 2\left\langle h^2 \right\rangle - 2\left\langle h(0, 0)h(x.y)\right\rangle = 2\sigma^2 - 2C(x, y)$$

where

$$C(x, y) = \sigma^2 e^{-(r/\xi)^{2h}}$$

Bounded correlations

If the correlations remain bounded as $r \to \infty$

$$g(x,y) = 2\left\langle h^2 \right\rangle - 2\left\langle h(0,0)h(x.y)\right\rangle = 2\sigma^2 - 2C(x,y)$$

where

$$C(x,y) = \sigma^2 e^{-(r/\xi)^{2h}}$$

$$\left(\frac{d\sigma}{d\Omega}\right) = \left(\frac{r_0\rho}{Q_z}\right)^2 \frac{A_0}{\sin\theta_1} e^{-Q_z^2\sigma^2} \int e^{Q_z^2 C(x,y)} e^{iQ_x x} e^{iQ_y y} dxdy$$

Bounded correlations

If the correlations remain bounded as $r \to \infty$

$$g(x,y) = 2\left\langle h^2 \right\rangle - 2\left\langle h(0,0)h(x.y) \right\rangle = 2\sigma^2 - 2C(x,y)$$

where

$$C(x,y) = \sigma^2 e^{-(r/\xi)^{2h}}$$

$$\begin{aligned}
\left(\frac{d\sigma}{d\Omega}\right) &= \left(\frac{r_0\rho}{Q_z}\right)^2 \frac{A_0}{\sin\theta_1} e^{-Q_z^2\sigma^2} \int e^{Q_z^2 C(x,y)} e^{iQ_x x} e^{iQ_y y} dxdy \\
&= \left(\frac{r_0\rho}{Q_z}\right)^2 \frac{A_0}{\sin\theta_1} e^{-Q_z^2\sigma^2} \int \left[e^{Q_z^2 C(x,y)} - 1 + 1\right] e^{iQ_x x} e^{iQ_y y} dxdy
\end{aligned}$$

Bounded correlations

If the correlations remain bounded as $r \to \infty$

$$g(x, y) = 2\left\langle h^2 \right\rangle - 2\left\langle h(0,0)h(x.y) \right\rangle = 2\sigma^2 - 2C(x, y)$$

where

$$C(x, y) = \sigma^2 e^{-(r/\xi)^{2h}}$$

$$\begin{aligned}
\left(\frac{d\sigma}{d\Omega}\right) &= \left(\frac{r_0\rho}{Q_z}\right)^2 \frac{A_0}{\sin\theta_1} e^{-Q_z^2\sigma^2} \int e^{Q_z^2 C(x,y)} e^{iQ_x x} e^{iQ_y y} dxdy \\
&= \left(\frac{r_0\rho}{Q_z}\right)^2 \frac{A_0}{\sin\theta_1} e^{-Q_z^2\sigma^2} \int \left[e^{Q_z^2 C(x,y)} - 1 + 1 \right] e^{iQ_x x} e^{iQ_y y} dxdy
\end{aligned}$$

Bounded correlations

If the correlations remain bounded as $r \to \infty$

$$g(x, y) = 2\left\langle h^2 \right\rangle - 2\left\langle h(0,0)h(x.y)\right\rangle = 2\sigma^2 - 2C(x, y)$$

where

$$C(x, y) = \sigma^2 e^{-(r/\xi)^{2h}}$$

$$\begin{aligned}
\left(\frac{d\sigma}{d\Omega}\right) &= \left(\frac{r_0\rho}{Q_z}\right)^2 \frac{A_0}{\sin\theta_1} e^{-Q_z^2\sigma^2} \int e^{Q_z^2 C(x,y)} e^{iQ_x x} e^{iQ_y y}\, dxdy \\
&= \left(\frac{r_0\rho}{Q_z}\right)^2 \frac{A_0}{\sin\theta_1} e^{-Q_z^2\sigma^2} \int \left[e^{Q_z^2 C(x,y)} - 1 + 1\right] e^{iQ_x x} e^{iQ_y y}\, dxdy \\
&= \left(\frac{d\sigma}{d\Omega}\right)_{Fresnel} e^{-Q_z^2\sigma^2} + \left(\frac{r_0\rho}{Q_z}\right)^2 \frac{A_0}{\sin\theta_1} e^{-Q_z^2\sigma^2} F_{diffuse}(\vec{Q})
\end{aligned}$$

Bounded correlations

If the correlations remain bounded as $r \to \infty$

$$g(x,y) = 2\left\langle h^2 \right\rangle - 2\left\langle h(0,0)h(x.y) \right\rangle = 2\sigma^2 - 2C(x,y)$$

where

$$C(x,y) = \sigma^2 e^{-(r/\xi)^{2h}}$$

$$\begin{aligned}
\left(\frac{d\sigma}{d\Omega}\right) &= \left(\frac{r_0\rho}{Q_z}\right)^2 \frac{A_0}{\sin\theta_1} e^{-Q_z^2\sigma^2} \int e^{Q_z^2 C(x,y)} e^{iQ_x x} e^{iQ_y y}\, dxdy \\
&= \left(\frac{r_0\rho}{Q_z}\right)^2 \frac{A_0}{\sin\theta_1} e^{-Q_z^2\sigma^2} \int \left[e^{Q_z^2 C(x,y)} - 1 + 1\right] e^{iQ_x x} e^{iQ_y y}\, dxdy \\
&= \left(\frac{d\sigma}{d\Omega}\right)_{Fresnel} e^{-Q_z^2\sigma^2} + \left(\frac{r_0\rho}{Q_z}\right)^2 \frac{A_0}{\sin\theta_1} e^{-Q_z^2\sigma^2} F_{diffuse}(\vec{Q})
\end{aligned}$$

And the scattering exhibits both a specular peak, reduced by uncorrelated roughness, and diffuse scattering from the correlated portion of the surface

Layering in liquid films

TEHOS, tetrakis–(2-ethylhexoxy)–silane, a non-polar, roughly spherical molecule, was deposited on Si(111) single crystals

C.-J. Yu et al., "Observation of molecular layering in thin liquid films using x-ray reflectivity", *Phys. Rev. Lett.* **82**, 2326–2329 (1999).

Layering in liquid films

TEHOS, tetrakis–(2-ethylhexoxy)–silane, a non-polar, roughly spherical molecule, was deposited on Si(111) single crystals

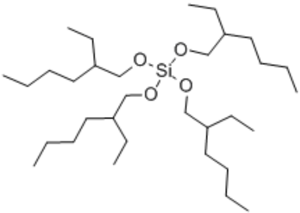

C.-J. Yu et al., "Observation of molecular layering in thin liquid films using x-ray reflectivity", *Phys. Rev. Lett.* **82**, 2326–2329 (1999).

Layering in liquid films

TEHOS, tetrakis–(2-ethylhexoxy)–silane,
a non-polar, roughly spherical molecule, was deposited on Si(111) single crystals

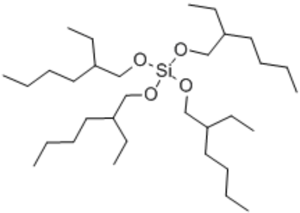

Specular reflection measurements were made at MRCAT (Sector 10 at APS) and at X18A (at NSLS).

C.-J. Yu et al., "Observation of molecular layering in thin liquid films using x-ray reflectivity", *Phys. Rev. Lett.* **82**, 2326–2329 (1999).

Layering in liquid films

TEHOS, tetrakis–(2-ethylhexoxy)–silane, a non-polar, roughly spherical molecule, was deposited on Si(111) single crystals

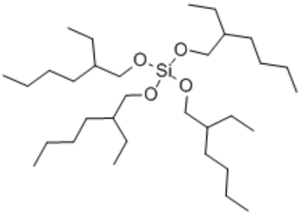

Specular reflection measurements were made at MRCAT (Sector 10 at APS) and at X18A (at NSLS).

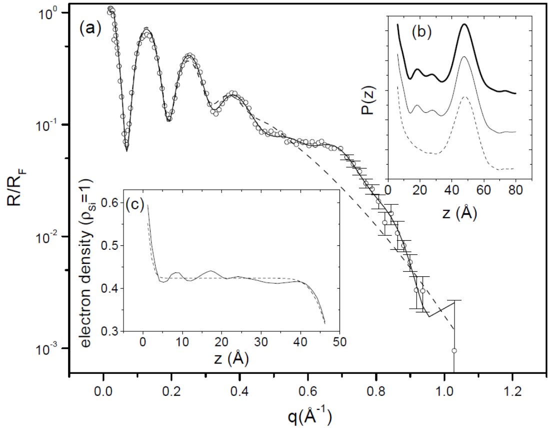

C.-J. Yu et al., "Observation of molecular layering in thin liquid films using x-ray reflectivity", *Phys. Rev. Lett.* **82**, 2326–2329 (1999).

Layering in liquid films

TEHOS, tetrakis–(2-ethylhexoxy)–silane, a non-polar, roughly spherical molecule, was deposited on Si(111) single crystals

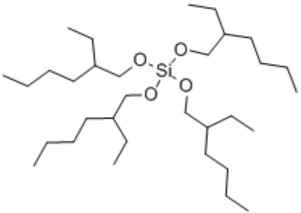

Specular reflection measurements were made at MRCAT (Sector 10 at APS) and at X18A (at NSLS).

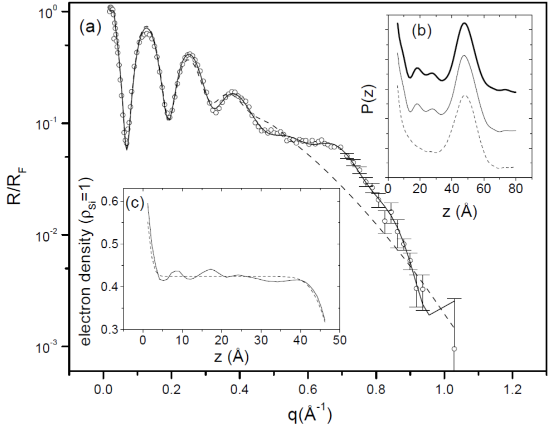

Deviations from uniform density are used to fit experimental reflectivity

C.-J. Yu et al., "Observation of molecular layering in thin liquid films using x-ray reflectivity", *Phys. Rev. Lett.* **82**, 2326–2329 (1999).

Layering in liquid films

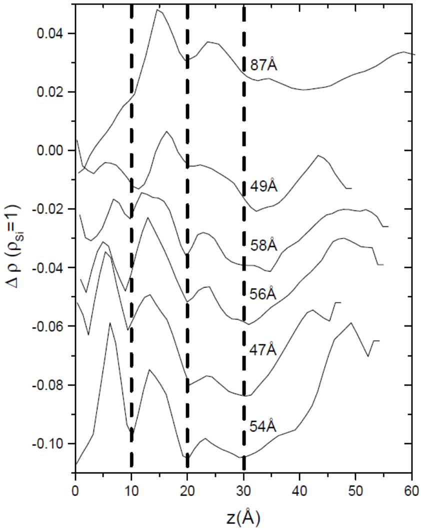

C.-J. Yu et al., "Observation of molecular layering in thin liquid films using x-ray reflectivity," *Phys. Rev. Lett.* **82**, 2326–2329 (1999).

Layering in liquid films

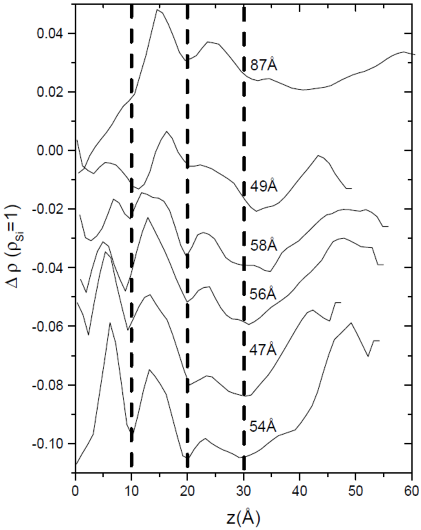

The peak below 10Å appears in all but the thickest film and depends on the interactions between film and substrate.

C.-J. Yu et al., "Observation of molecular layering in thin liquid films using x-ray reflectivity," *Phys. Rev. Lett.* **82**, 2326–2329 (1999).

Layering in liquid films

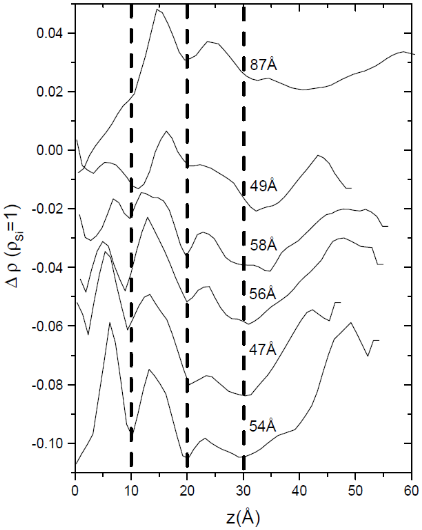

The peak below 10Å appears in all but the thickest film and depends on the interactions between film and substrate.

There are always peaks between 10-20Å and 20-30Åand a broad peak at the free surface showing the presence of ordered layers of molecules.

C.-J. Yu et al., "Observation of molecular layering in thin liquid films using x-ray reflectivity," *Phys. Rev. Lett.* **82**, 2326–2329 (1999).

Layering in liquid films

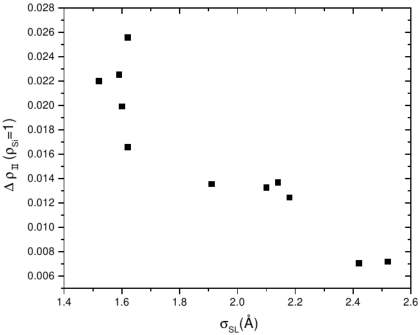

As the surface layer thickens, the deviation of density from the average decreases

The peak below 10Å appears in all but the thickest film and depends on the interactions between film and substrate.

There are always peaks between 10-20Å and 20-30Åand a broad peak at the free surface showing the presence of ordered layers of molecules.

C.-J. Yu et al., "Observation of molecular layering in thin liquid films using x-ray reflectivity," *Phys. Rev. Lett.* **82**, 2326–2329 (1999).

Layering in liquid films

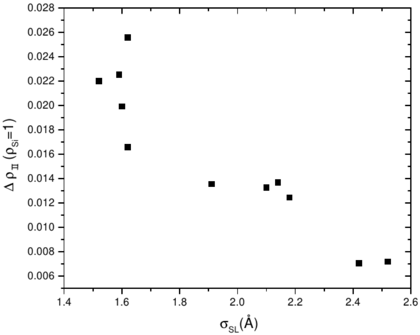

As the surface layer thickens, the deviation of density from the average decreases

The peak below 10Å appears in all but the thickest film and depends on the interactions between film and substrate.

There are always peaks between 10-20Å and 20-30Åand a broad peak at the free surface showing the presence of ordered layers of molecules.

The authors conclude that the presence of a hard smooth surface is required for ordering and therefore deviations from an ideal, isotropic liquid.

C.-J. Yu et al., "Observation of molecular layering in thin liquid films using x-ray reflectivity," *Phys. Rev. Lett.* **82**, 2326–2329 (1999).

Film growth kinetics

The goal of this project was to understand the evolution of surface roughness during the growth of a silver thin film.

C. Thompson et al., "X-ray-reflectivity study of the growth kinetics of vapor-deposited silver films," *Phys. Rev. B* **49**, 4902–4907 (1994).

Film growth kinetics

The goal of this project was to understand the evolution of surface roughness during the growth of a silver thin film.

The question is whether there is surface diffusion of the deposited atoms during the growth

C. Thompson et al., "X-ray-reflectivity study of the growth kinetics of vapor-deposited silver films," *Phys. Rev. B* **49**, 4902–4907 (1994).

Film growth kinetics

The goal of this project was to understand the evolution of surface roughness during the growth of a silver thin film.

The question is whether there is surface diffusion of the deposited atoms during the growth

In order to study this question, a silicon substrate was placed in the growth chamber and illuminated with x-rays after a period of deposition

C. Thompson et al., "X-ray-reflectivity study of the growth kinetics of vapor-deposited silver films," *Phys. Rev. B* **49**, 4902–4907 (1994).

Film growth kinetics

The goal of this project was to understand the evolution of surface roughness during the growth of a silver thin film.

The question is whether there is surface diffusion of the deposited atoms during the growth

In order to study this question, a silicon substrate was placed in the growth chamber and illuminated with x-rays after a period of deposition

The sample was flipped to a downward facing position and silver atoms deposited for a period of time, then flipped to an upward facing position for the reflectivity measurements

C. Thompson et al., "X-ray-reflectivity study of the growth kinetics of vapor-deposited silver films," *Phys. Rev. B* **49**, 4902–4907 (1994).

Film growth kinetics

The goal of this project was to understand the evolution of surface roughness during the growth of a silver thin film.

The question is whether there is surface diffusion of the deposited atoms during the growth

In order to study this question, a silicon substrate was placed in the growth chamber and illuminated with x-rays after a period of deposition

The sample was flipped to a downward facing position and silver atoms deposited for a period of time, then flipped to an upward facing position for the reflectivity measurements

5 deposition with thicknesses varying from 10 nm to 150 nm were studies

C. Thompson et al., "X-ray-reflectivity study of the growth kinetics of vapor-deposited silver films," *Phys. Rev. B* **49**, 4902–4907 (1994).

Film growth kinetics

Gaussian roughness profile with a "roughness" exponent $0 < h < 1$.

C. Thompson et al., "X-ray-reflectivity study of the growth kinetics of vapor-deposited silver films," *Phys. Rev. B* **49**, 4902–4907 (1994).

Film growth kinetics

Gaussian roughness profile with a "roughness" exponent $0 < h < 1$.

$g(r) \propto r^{2h}$

C. Thompson et al., "X-ray-reflectivity study of the growth kinetics of vapor-deposited silver films," *Phys. Rev. B* **49**, 4902–4907 (1994).

Film growth kinetics

Gaussian roughness profile with a "roughness" exponent $0 < h < 1$. As the film is grown by vapor deposition, the rms width σ, grows with a "growth exponent" β

$$g(r) \propto r^{2h}$$

C. Thompson et al., "X-ray-reflectivity study of the growth kinetics of vapor-deposited silver films," *Phys. Rev. B* **49**, 4902–4907 (1994).

Film growth kinetics

Gaussian roughness profile with a "roughness" exponent $0 < h < 1$. As the film is grown by vapor deposition, the rms width σ, grows with a "growth exponent" β

$$g(r) \propto r^{2h} \qquad \sigma \propto t^{\beta}$$

C. Thompson et al., "X-ray-reflectivity study of the growth kinetics of vapor-deposited silver films," *Phys. Rev. B* **49**, 4902–4907 (1994).

Film growth kinetics

Gaussian roughness profile with a "roughness" exponent $0 < h < 1$. As the film is grown by vapor deposition, the rms width σ, grows with a "growth exponent" β and the correlation length in the plane of the surface, ξ evolves with the "dynamic" scaling exponent, $z_s = h/\beta$.

$$g(r) \propto r^{2h} \qquad \sigma \propto t^{\beta}$$

C. Thompson et al., "X-ray-reflectivity study of the growth kinetics of vapor-deposited silver films," *Phys. Rev. B* **49**, 4902–4907 (1994).

Film growth kinetics

Gaussian roughness profile with a "roughness" exponent $0 < h < 1$. As the film is grown by vapor deposition, the rms width σ, grows with a "growth exponent" β and the correlation length in the plane of the surface, ξ evolves with the "dynamic" scaling exponent, $z_s = h/\beta$.

$$g(r) \propto r^{2h} \qquad \sigma \propto t^{\beta}$$

$$\xi \propto t^{1/z_s}$$

$h \approx 0.33$, $\beta \approx 0.25$ for no diffusion.

C. Thompson et al., "X-ray-reflectivity study of the growth kinetics of vapor-deposited silver films," *Phys. Rev. B* **49**, 4902–4907 (1994).

Film growth kinetics

Gaussian roughness profile with a "roughness" exponent $0 < h < 1$. As the film is grown by vapor deposition, the rms width σ, grows with a "growth exponent" β and the correlation length in the plane of the surface, ξ evolves with the "dynamic" scaling exponent, $z_s = h/\beta$.

$$g(r) \propto r^{2h} \qquad \sigma \propto t^{\beta}$$

$$\xi \propto t^{1/z_s} \qquad \langle h \rangle \propto t$$

$h \approx 0.33$, $\beta \approx 0.25$ for no diffusion.

C. Thompson et al., "X-ray-reflectivity study of the growth kinetics of vapor-deposited silver films," *Phys. Rev. B* **49**, 4902–4907 (1994).

Film growth kinetics

Gaussian roughness profile with a "roughness" exponent $0 < h < 1$. As the film is grown by vapor deposition, the rms width σ, grows with a "growth exponent" β and the correlation length in the plane of the surface, ξ evolves with the "dynamic" scaling exponent, $z_s = h/\beta$.

$$g(r) \propto r^{2h} \qquad \sigma \propto t^{\beta}$$

$$\xi \propto t^{1/z_s} \qquad \langle h \rangle \propto t$$

$h \approx 0.33$, $\beta \approx 0.25$ for no diffusion.

Ag/Si films: 10nm (A), 18nm (B), 37nm (C), 73nm (D), 150nm (E)

C. Thompson et al., "X-ray-reflectivity study of the growth kinetics of vapor-deposited silver films," *Phys. Rev. B* **49**, 4902–4907 (1994).

Film growth kinetics

Gaussian roughness profile with a "roughness" exponent $0 < h < 1$. As the film is grown by vapor deposition, the rms width σ, grows with a "growth exponent" β and the correlation length in the plane of the surface, ξ evolves with the "dynamic" scaling exponent, $z_s = h/\beta$.

$$g(r) \propto r^{2h} \qquad \sigma \propto t^{\beta}$$

$$\xi \propto t^{1/z_s} \qquad \langle h \rangle \propto t$$

$h \approx 0.33$, $\beta \approx 0.25$ for no diffusion.

Ag/Si films: 10nm (A), 18nm (B), 37nm (C), 73nm (D), 150nm (E)

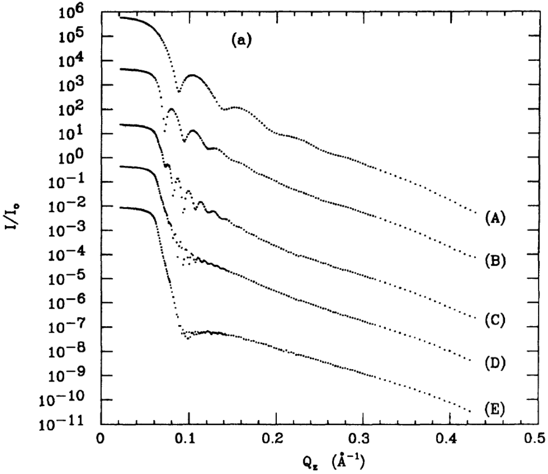

C. Thompson et al., "X-ray-reflectivity study of the growth kinetics of vapor-deposited silver films," *Phys. Rev. B* **49**, 4902–4907 (1994).

Film growth kinetics

Gaussian roughness profile with a "roughness" exponent $0 < h < 1$. As the film is grown by vapor deposition, the rms width σ, grows with a "growth exponent" β and the correlation length in the plane of the surface, ξ evolves with the "dynamic" scaling exponent, $z_s = h/\beta$.

$$g(r) \propto r^{2h} \qquad \sigma \propto t^{\beta}$$

$$\xi \propto t^{1/z_s} \qquad \langle h \rangle \propto t$$

$h \approx 0.33$, $\beta \approx 0.25$ for no diffusion.

Ag/Si films: 10nm (A), 18nm (B), 37nm (C), 73nm (D), 150nm (E)

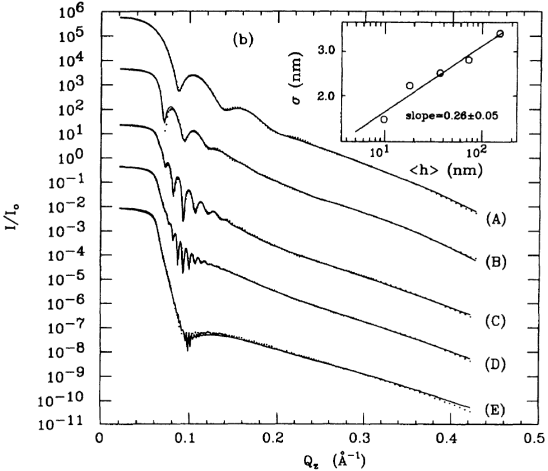

C. Thompson et al., "X-ray-reflectivity study of the growth kinetics of vapor-deposited silver films," *Phys. Rev. B* **49**, 4902–4907 (1994).

Film growth kinetics

h can be obtained from the diffuse off-specular reflection which should vary as

Film growth kinetics

h can be obtained from the diffuse off-specular reflection which should vary as

$$I(q_z) \propto \sigma^{-2/h} q_z^{-(3+1/h)}$$

Film growth kinetics

h can be obtained from the diffuse off-specular reflection which should vary as

$$I(q_z) \propto \sigma^{-2/h} q_z^{-(3+1/h)}$$

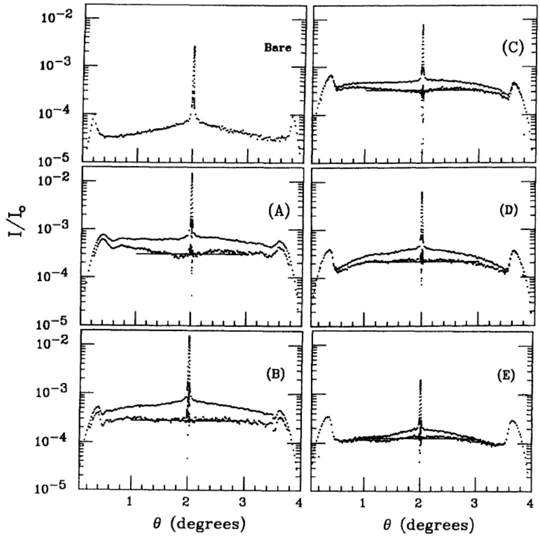

Film growth kinetics

h can be obtained from the diffuse off-specular reflection which should vary as

$$I(q_z) \propto \sigma^{-2/h} q_z^{-(3+1/h)}$$

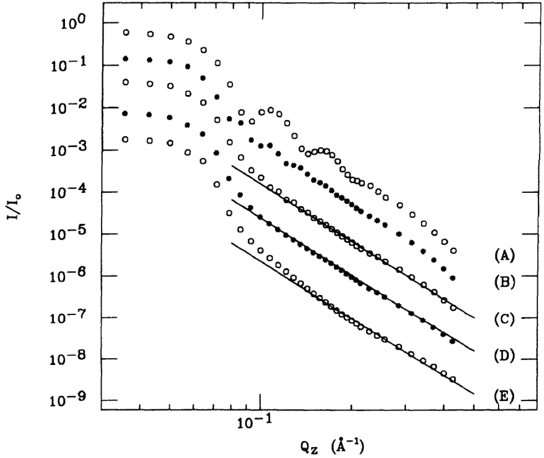

Film growth kinetics

h can be obtained from the diffuse off-specular reflection which should vary as

$$I(q_z) \propto \sigma^{-2/h} q_z^{-(3+1/h)}$$

This gives $h = 0.63$ but is this correct?

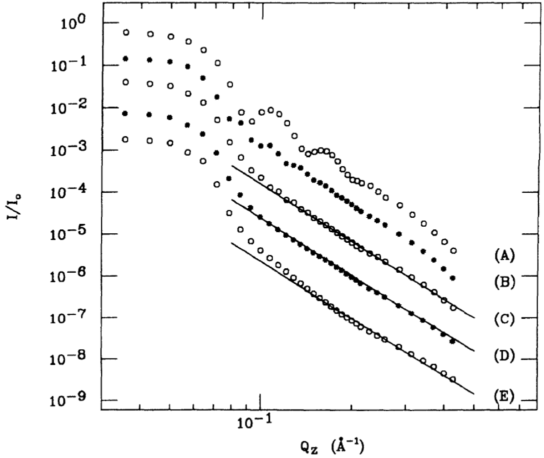

Film growth kinetics

h can be obtained from the diffuse off-specular reflection which should vary as

$$I(q_z) \propto \sigma^{-2/h} q_z^{-(3+1/h)}$$

This gives $h = 0.63$ but is this correct?

Measure it directly using STM

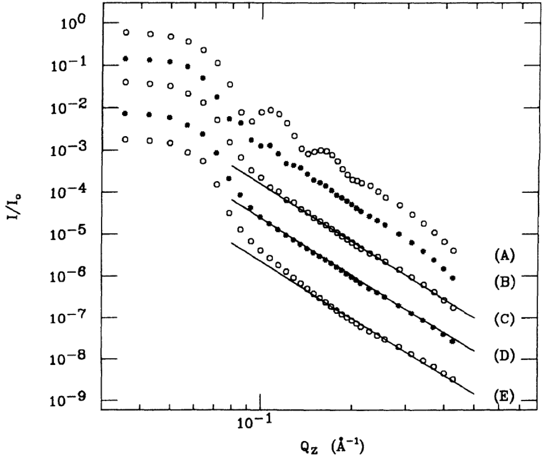

Film growth kinetics

h can be obtained from the diffuse off-specular reflection which should vary as

$$I(q_z) \propto \sigma^{-2/h} q_z^{-(3+1/h)}$$

This gives $h = 0.63$ but is this correct?

Measure it directly using STM

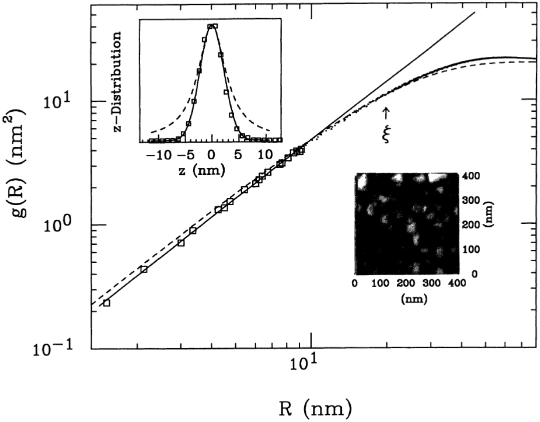

Film growth kinetics

h can be obtained from the diffuse off-specular reflection which should vary as

$$I(q_z) \propto \sigma^{-2/h} q_z^{-(3+1/h)}$$

This gives $h = 0.63$ but is this correct?

Measure it directly using STM

$$g(r) = 2\sigma^2 \left[1 - e^{(r/\xi)^{2h}}\right]$$

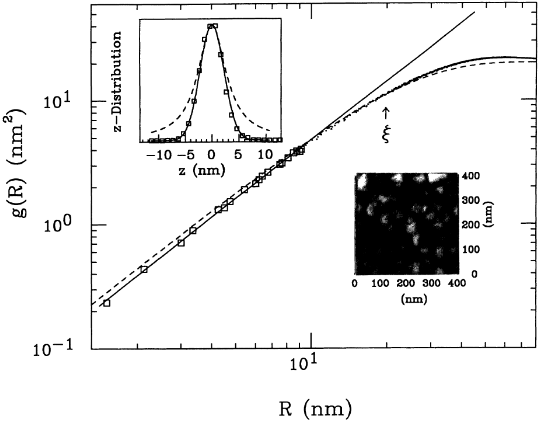

Film growth kinetics

h can be obtained from the diffuse off-specular reflection which should vary as

$$I(q_z) \propto \sigma^{-2/h} q_z^{-(3+1/h)}$$

This gives $h = 0.63$ but is this correct?

Measure it directly using STM

$$g(r) = 2\sigma^2 \left[1 - e^{(r/\xi)^{2h}}\right]$$

$$h = 0.78, \quad \xi = 23\text{nm}, \quad \sigma = 3.2\text{nm}$$

Thus $z_s = h/\beta = 2.7$

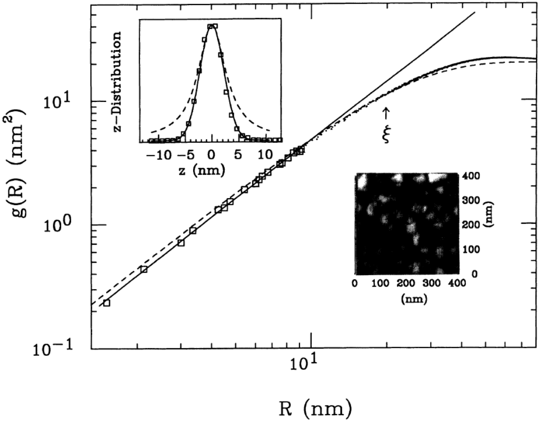

Film growth kinetics

h can be obtained from the diffuse off-specular reflection which should vary as

$$I(q_z) \propto \sigma^{-2/h} q_z^{-(3+1/h)}$$

This gives $h = 0.63$ but is this correct?

Measure it directly using STM

$$g(r) = 2\sigma^2 \left[1 - e^{(r/\xi)^{2h}} \right]$$

$$h = 0.78, \quad \xi = 23\text{nm}, \quad \sigma = 3.2\text{nm}$$

Thus $z_s = h/\beta = 2.7$

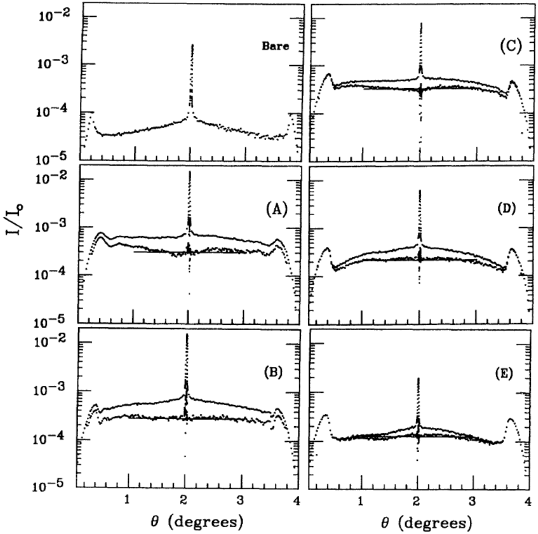

Film growth kinetics

h can be obtained from the diffuse off-specular reflection which should vary as

$$I(q_z) \propto \sigma^{-2/h} q_z^{-(3+1/h)}$$

This gives $h = 0.63$ but is this correct?

Measure it directly using STM

$$g(r) = 2\sigma^2 \left[1 - e^{(r/\xi)^{2h}}\right]$$

$$h = 0.78, \quad \xi = 23\text{nm}, \quad \sigma = 3.2\text{nm}$$

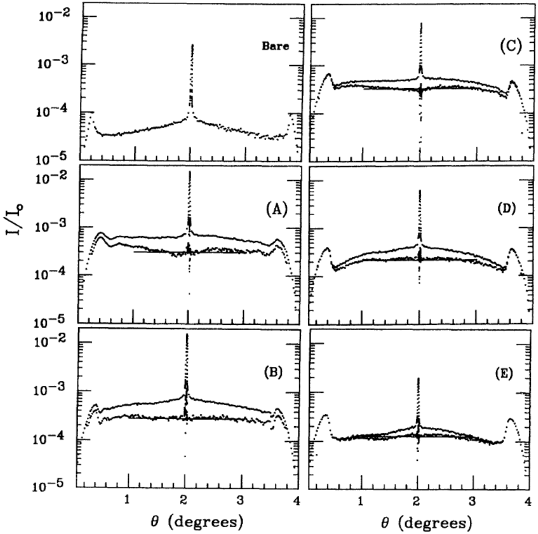

Thus $z_s = h/\beta = 2.7$ and diffraction data confirm $\xi = 19.9\langle h\rangle^{1/2.7}$ Å

Liquid metal surfaces

X-ray reflectivity using synchrotron radiation has made possible the study of the surface of liquid metals

P. Pershan, "Review of the highlights of x-ray studies of liquid metal surfaces," *J. Appl. Phys.* **116**, 222201 (2014).

Liquid metal surfaces

X-ray reflectivity using synchrotron radiation has made possible the study of the surface of liquid metals

a liquid can be described as charged ions in a sea of conduction electrons

P. Pershan, "Review of the highlights of x-ray studies of liquid metal surfaces," *J. Appl. Phys.* **116**, 222201 (2014).

Liquid metal surfaces

X-ray reflectivity using synchrotron radiation has made possible the study of the surface of liquid metals

a liquid can be described as charged ions in a sea of conduction electrons

this leads to a well-defined surface structure as can be seen in liquid gallium

P. Pershan, "Review of the highlights of x-ray studies of liquid metal surfaces," *J. Appl. Phys.* **116**, 222201 (2014).

Liquid metal surfaces

X-ray reflectivity using synchrotron radiation has made possible the study of the surface of liquid metals

a liquid can be described as charged ions in a sea of conduction electrons

this leads to a well-defined surface structure as can be seen in liquid gallium

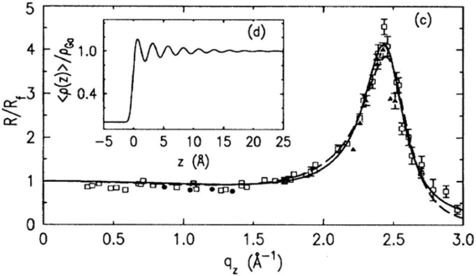

P. Pershan, "Review of the highlights of x-ray studies of liquid metal surfaces," *J. Appl. Phys.* **116**, 222201 (2014).

Liquid metal surfaces

X-ray reflectivity using synchrotron radiation has made possible the study of the surface of liquid metals

a liquid can be described as charged ions in a sea of conduction electrons

this leads to a well-defined surface structure as can be seen in liquid gallium

contrast this with the scattering from liquid mercury

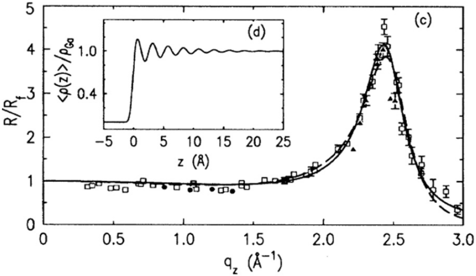

P. Pershan, "Review of the highlights of x-ray studies of liquid metal surfaces," *J. Appl. Phys.* **116**, 222201 (2014).

Liquid metal surfaces

X-ray reflectivity using synchrotron radiation has made possible the study of the surface of liquid metals

a liquid can be described as charged ions in a sea of conduction electrons

this leads to a well-defined surface structure as can be seen in liquid gallium

contrast this with the scattering from liquid mercury

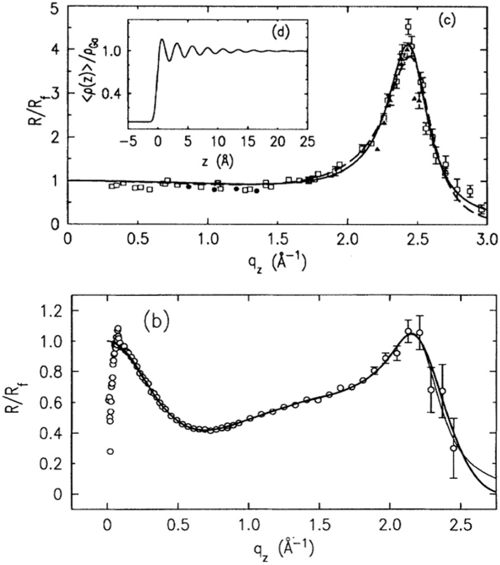

P. Pershan, "Review of the highlights of x-ray studies of liquid metal surfaces," *J. Appl. Phys.* **116**, 222201 (2014).

Liquid metal eutectics

High vapor pressure and thermal excitations limit the number of pure metals which can be studied but alloy eutectics provide many possibilities

O. Shpyrko *et al.*, "Atomic-scale surface demixing in a eutectic liquid BiSn alloy," *Phys. Rev. Lett.* **95**, 106103 (2005).

Liquid metal eutectics

High vapor pressure and thermal excitations limit the number of pure metals which can be studied but alloy eutectics provide many possibilities

tune x-rays around the Bi absorption edge at 13.42 keV and measure a $Bi_{43}Sn_{57}$ eutectic

O. Shpyrko *et al.*, "Atomic-scale surface demixing in a eutectic liquid BiSn alloy," *Phys. Rev. Lett.* **95**, 106103 (2005).

Liquid metal eutectics

High vapor pressure and thermal excitations limit the number of pure metals which can be studied but alloy eutectics provide many possibilities

tune x-rays around the Bi absorption edge at 13.42 keV and measure a $Bi_{43}Sn_{57}$ eutectic

O. Shpyrko *et al.*, "Atomic-scale surface demixing in a eutectic liquid BiSn alloy," *Phys. Rev. Lett.* **95**, 106103 (2005).

Liquid metal eutectics

High vapor pressure and thermal excitations limit the number of pure metals which can be studied but alloy eutectics provide many possibilities

tune x-rays around the Bi absorption edge at 13.42 keV and measure a $Bi_{43}Sn_{57}$ eutectic

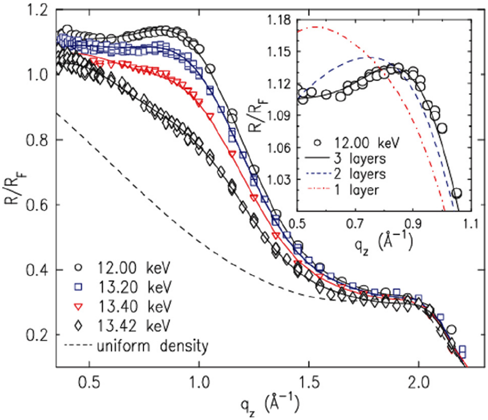

O. Shpyrko *et al.*, "Atomic-scale surface demixing in a eutectic liquid BiSn alloy," *Phys. Rev. Lett.* **95**, 106103 (2005).

Liquid metal eutectics

High vapor pressure and thermal excitations limit the number of pure metals which can be studied but alloy eutectics provide many possibilities

tune x-rays around the Bi absorption edge at 13.42 keV and measure a $Bi_{43}Sn_{57}$ eutectic

surface layer is rich in Bi (95%), second layer is deficient (25%), and third layer is rich in Bi (53%) once again

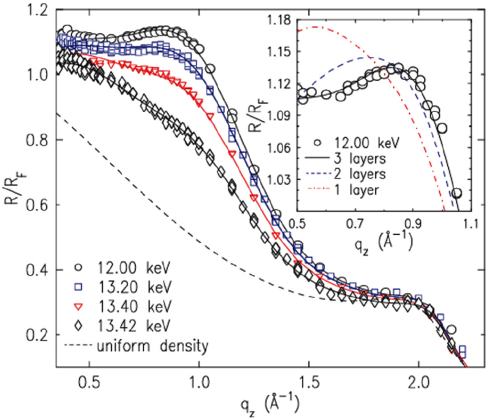

O. Shpyrko *et al.*, "Atomic-scale surface demixing in a eutectic liquid BiSn alloy," *Phys. Rev. Lett.* **95**, 106103 (2005).

Tangential focusing mirror

The shape of an ideal mirror is an ellipse, where any ray coming from one focus will be projected to the second focus.

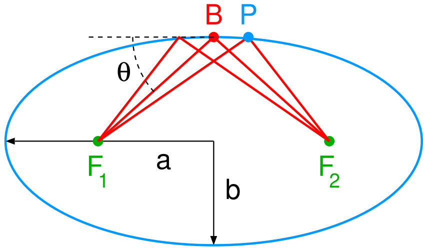

Tangential focusing mirror

The shape of an ideal mirror is an ellipse, where any ray coming from one focus will be projected to the second focus. Consider a 1:1 focusing mirror. For an ellipse the sum of the distances from any point on the ellipse to the foci is a constant.

$$F_1P + F_2P = 2a$$

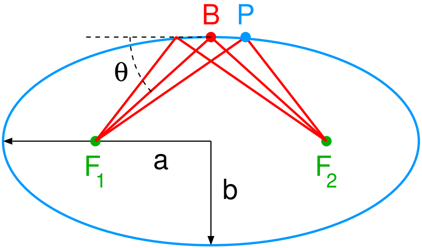

Tangential focusing mirror

The shape of an ideal mirror is an ellipse, where any ray coming from one focus will be projected to the second focus. Consider a 1:1 focusing mirror. For an ellipse the sum of the distances from any point on the ellipse to the foci is a constant.

$$F_1P + F_2P = 2a$$

$$F_1B = F_2B = a$$

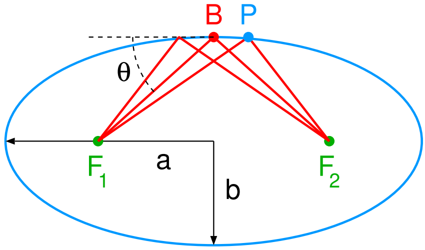

Tangential focusing mirror

The shape of an ideal mirror is an ellipse, where any ray coming from one focus will be projected to the second focus. Consider a 1:1 focusing mirror. For an ellipse the sum of the distances from any point on the ellipse to the foci is a constant.

$$F_1P + F_2P = 2a$$

$$F_1B = F_2B = a$$

$$\sin\theta = \frac{b}{a}$$

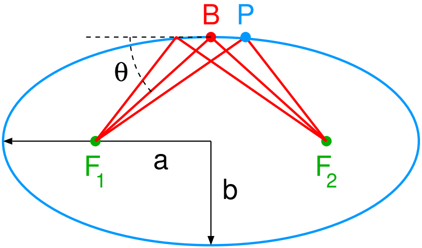

Tangential focusing mirror

The shape of an ideal mirror is an ellipse, where any ray coming from one focus will be projected to the second focus. Consider a 1:1 focusing mirror. For an ellipse the sum of the distances from any point on the ellipse to the foci is a constant.

$$F_1P + F_2P = 2a$$

$$F_1B = F_2B = a$$

$$\sin\theta = \frac{b}{a}$$

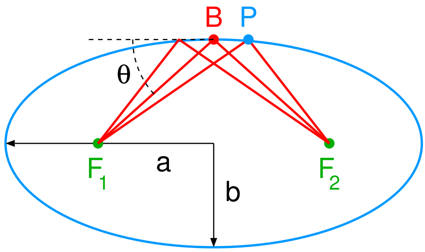

$$\frac{1}{f} = \frac{1}{o} + \frac{1}{i}$$

Tangential focusing mirror

The shape of an ideal mirror is an ellipse, where any ray coming from one focus will be projected to the second focus. Consider a 1:1 focusing mirror. For an ellipse the sum of the distances from any point on the ellipse to the foci is a constant.

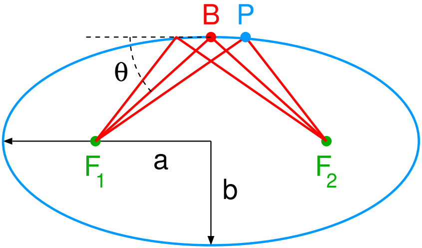

$$F_1P + F_2P = 2a$$

$$F_1B = F_2B = a$$

$$\sin\theta = \frac{b}{a}$$

$$\frac{1}{f} = \frac{1}{o} + \frac{1}{i} = \frac{2}{a}$$

$$f = \frac{a}{2}$$

Tangential focusing mirror

The shape of an ideal mirror is an ellipse, where any ray coming from one focus will be projected to the second focus. Consider a 1:1 focusing mirror. For an ellipse the sum of the distances from any point on the ellipse to the foci is a constant.

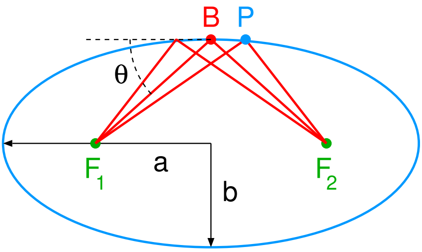

$$F_1P + F_2P = 2a$$

$$F_1B = F_2B = a$$

$$\sin\theta = \frac{b}{a} = \frac{b}{2f}$$

$$\frac{1}{f} = \frac{1}{o} + \frac{1}{i} = \frac{2}{a}$$

$$f = \frac{a}{2}$$

Saggital focusing mirror

Ellipses are hard figures to make, so usually, they are approximated by circles. In the case of saggital focusing, an ellipsoid of revolution with diameter $2b$, is used for focusing.

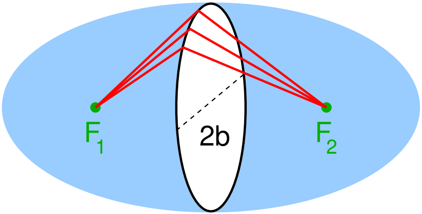

Saggital focusing mirror

Ellipses are hard figures to make, so usually, they are approximated by circles. In the case of saggital focusing, an ellipsoid of revolution with diameter $2b$, is used for focusing.

$$\rho_{saggital} = b = 2f \sin\theta$$

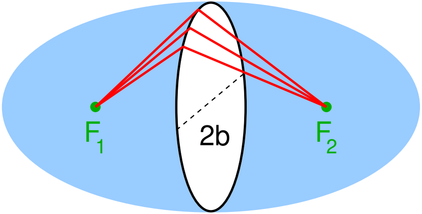

Saggital focusing mirror

Ellipses are hard figures to make, so usually, they are approximated by circles. In the case of saggital focusing, an ellipsoid of revolution with diameter $2b$, is used for focusing.

$$\rho_{saggital} = b = 2f \sin\theta$$

The tangential focus is also usually approximated by a circular cross-section with radius

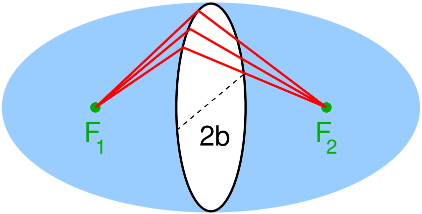

Saggital focusing mirror

Ellipses are hard figures to make, so usually, they are approximated by circles. In the case of saggital focusing, an ellipsoid of revolution with diameter $2b$, is used for focusing.

$$\rho_{saggital} = b = 2f \sin\theta$$

The tangential focus is also usually approximated by a circular cross-section with radius

$$\rho_{tangential} = a = \frac{2f}{\sin\theta}$$

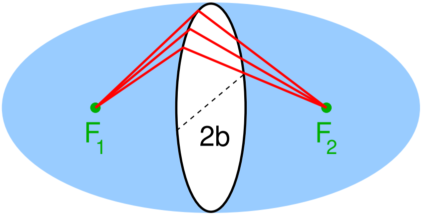

Types of focusing mirrors

A simple mirror such as the one at MRCAT consists of a polished glass slab with two "legs".

Types of focusing mirrors

A simple mirror such as the one at MRCAT consists of a polished glass slab with two "legs". A force is applied mechanically to push the legs apart and bend the mirror to a radius as small as $R = 500$m.

Types of focusing mirrors

A simple mirror such as the one at MRCAT consists of a polished glass slab with two "legs". A force is applied mechanically to push the legs apart and bend the mirror to a radius as small as $R = 500$m.

The bimorph mirror is designed to obtain a smaller form error than a simple bender through the use of multiple actuators tuned experimentally.

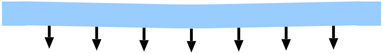

Types of focusing mirrors

A simple mirror such as the one at MRCAT consists of a polished glass slab with two “legs”. A force is applied mechanically to push the legs apart and bend the mirror to a radius as small as $R = 500$m.

The bimorph mirror is designed to obtain a smaller form error than a simple bender through the use of multiple actuators tuned experimentally.

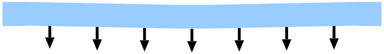

A cost effective way to focus in both directions is a toroidal mirror which has a fixed bend in the transverse direction but which can be bent longitudinally to change the vertical focus.

Dual focusing options

Dual focusing options

- Toroidal mirror — simple, moderate focus, good for initial focusing element, easy to distort beam

Dual focusing options

- Toroidal mirror — simple, moderate focus, good for initial focusing element, easy to distort beam
- Saggittal focusing crystal & vertical focusing mirror — adjustable in both directions, good for initial focusing element

Dual focusing options

- Toroidal mirror — simple, moderate focus, good for initial focusing element, easy to distort beam
- Saggittal focusing crystal & vertical focusing mirror — adjustable in both directions, good for initial focusing element
- Kirkpatrick-Baez mirror pair — in combination with an initial focusing element, good for final small focal spot and variable energy

Dual focusing options

- Toroidal mirror — simple, moderate focus, good for initial focusing element, easy to distort beam
- Saggittal focusing crystal & vertical focusing mirror — adjustable in both directions, good for initial focusing element
- Kirkpatrick-Baez mirror pair — in combination with an initial focusing element, good for final small focal spot and variable energy
- Zone plates — in combination with an initial focusing element, gives smallest focal spot, but hard to vary energy

Dual focusing options

- Toroidal mirror — simple, moderate focus, good for initial focusing element, easy to distort beam
- Saggittal focusing crystal & vertical focusing mirror — adjustable in both directions, good for initial focusing element
- Kirkpatrick-Baez mirror pair — in combination with an initial focusing element, good for final small focal spot and variable energy
- Zone plates — in combination with an initial focusing element, gives smallest focal spot, but hard to vary energy
- Refractive lenses — good final focus, focus moves with energy, significant attenuation and hard to change focal length

The MRCAT mirror

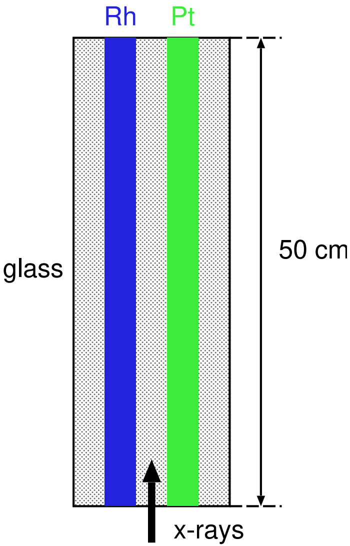

The MRCAT mirror

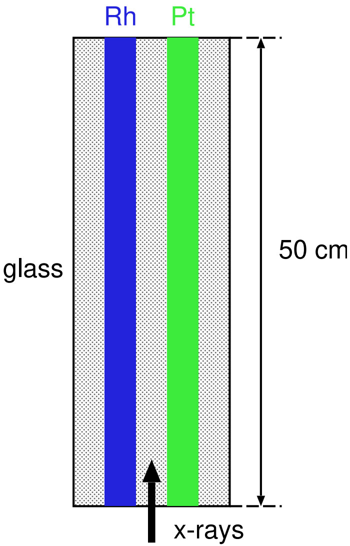

Ultra low expansion glass polished to a few Å roughness

The MRCAT mirror

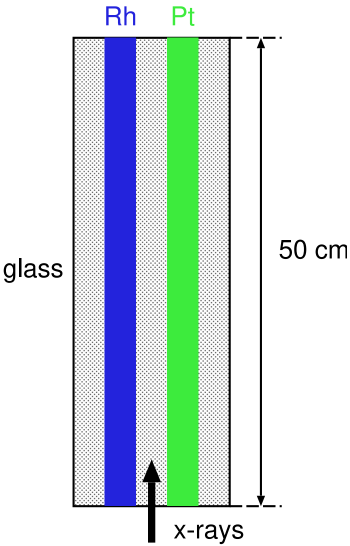

Ultra low expansion glass polished to a few Å roughness

One platinum stripe and one rhodium stripe deposited along the length of the mirror on top of a chromium buffer layer

The MRCAT mirror

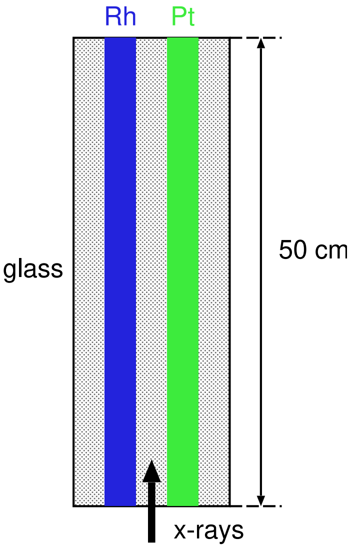

Ultra low expansion glass polished to a few Å roughness

One platinum stripe and one rhodium stripe deposited along the length of the mirror on top of a chromium buffer layer

A mounting system which permits angular positioning to less than 1/100 of a degree as well as horizontal and vertical motions

The MRCAT mirror

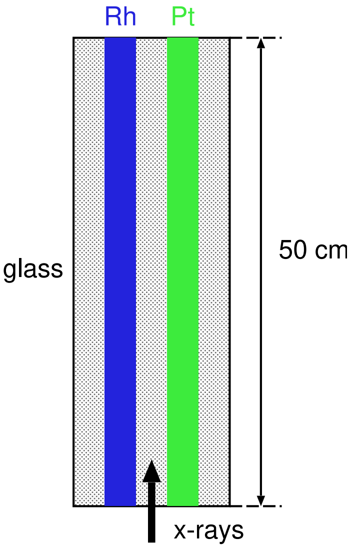

Ultra low expansion glass polished to a few Å roughness

One platinum stripe and one rhodium stripe deposited along the length of the mirror on top of a chromium buffer layer

A mounting system which permits angular positioning to less than 1/100 of a degree as well as horizontal and vertical motions

A bending mechanism to permit vertical focusing of the beam to $\sim 60\ \mu\text{m}$

Mirror performance

When illuminated with 12 keV x-rays on the glass "stripe", the reflectivity is measured as:

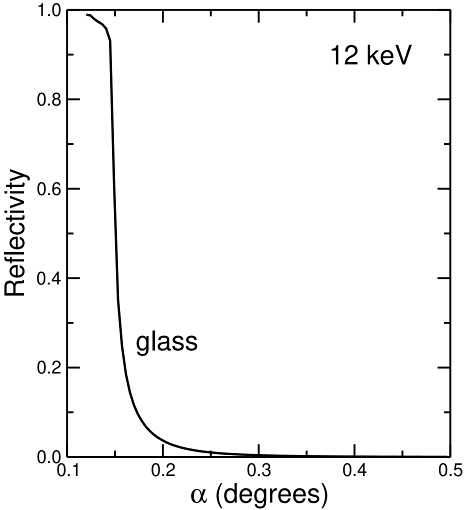

Mirror performance

When illuminated with 12 keV x-rays on the glass “stripe”, the reflectivity is measured as:

With the Rh stripe, the thin slab reflection is evident and the critical angle is significantly higher.

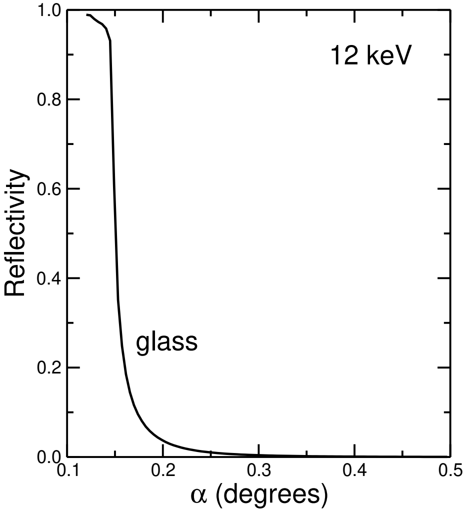

Mirror performance

When illuminated with 12 keV x-rays on the glass "stripe", the reflectivity is measured as:

With the Rh stripe, the thin slab reflection is evident and the critical angle is significantly higher.

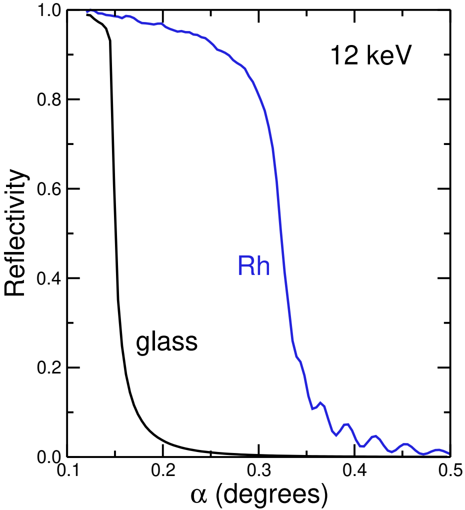

Mirror performance

When illuminated with 12 keV x-rays on the glass "stripe", the reflectivity is measured as:

With the Rh stripe, the thin slab reflection is evident and the critical angle is significantly higher.

The Pt stripe gives a higher critical angle still but a lower reflectivity and it looks like an infinite slab.

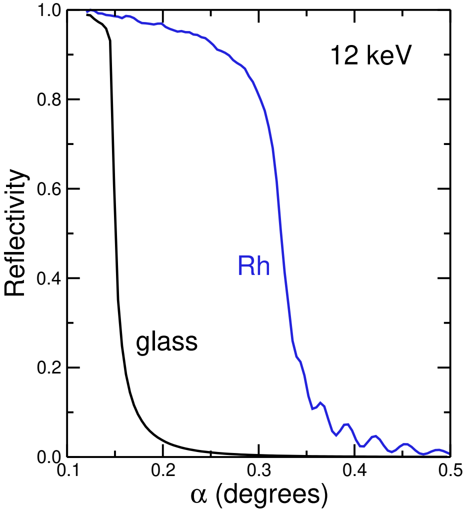

Mirror performance

When illuminated with 12 keV x-rays on the glass "stripe", the reflectivity is measured as:

With the Rh stripe, the thin slab reflection is evident and the critical angle is significantly higher.

The Pt stripe gives a higher critical angle still but a lower reflectivity and it looks like an infinite slab.

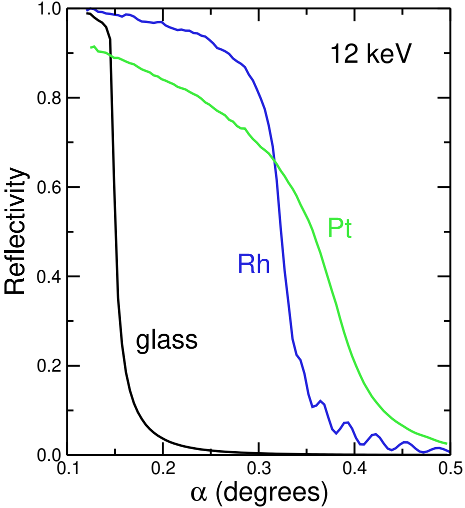

Mirror performance

When illuminated with 12 keV x-rays on the glass "stripe", the reflectivity is measured as:

With the Rh stripe, the thin slab reflection is evident and the critical angle is significantly higher.

The Pt stripe gives a higher critical angle still but a lower reflectivity and it looks like an infinite slab. Why?

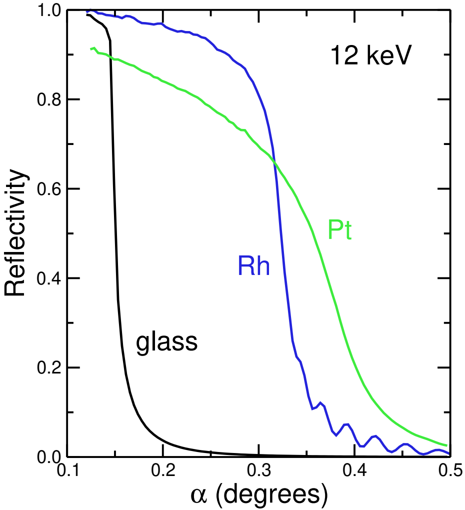

Mirror performance (cont.)

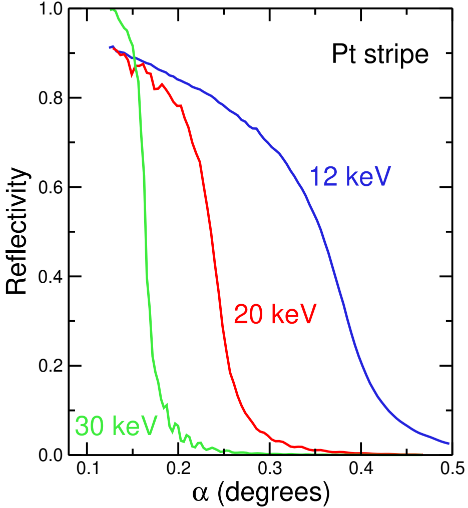

Mirror performance (cont.)

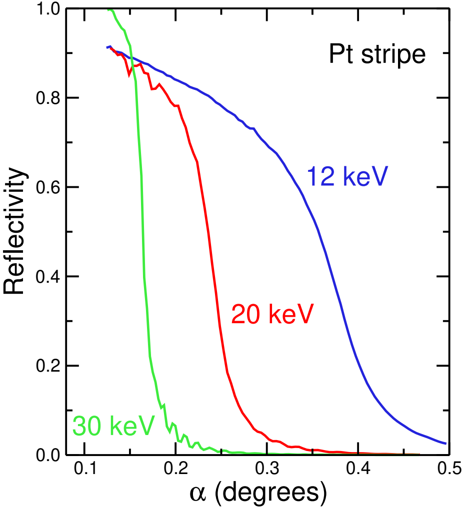

As we move up in energy the critical angle for the Pt stripe drops.

Mirror performance (cont.)

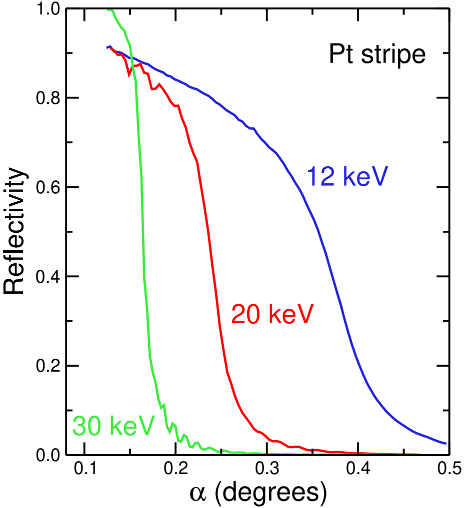

As we move up in energy the critical angle for the Pt stripe drops.

The reflectivity at low angles improves as we are well away from the Pt absorption edges at 11,565 eV, 13,273 eV, and 13,880 eV.

Mirror performance (cont.)

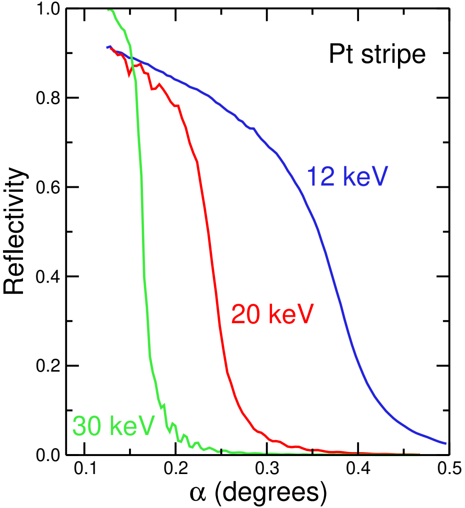

As we move up in energy the critical angle for the Pt stripe drops.

The reflectivity at low angles improves as we are well away from the Pt absorption edges at 11,565 eV, 13,273 eV, and 13,880 eV.

As energy rises, the Pt layer begins to show the reflectivity of a thin slab.